Near real-time agriculture monitoring at national scale at parcel resolution: Performance assessment of the Sen2-Agri automated system in various cropping systems around the world

Pierre Defourny, Sophie Bontemps, Nicolas Bellemans, Cosmin Cara, Gérard
Dedieu, Eric Guzzonato, Olivier Hagolle, Jordi Inglada, Laurentiu Nicola,
Thierry Rabaute, et al.

▶ **To cite this version:**

HAL Id: hal-03138321
https://hal.inrae.fr/hal-03138321

Submitted on 11 Feb 2021

Near real-time agriculture monitoring at national scale at parcel resolution: Performance assessment of the Sen2-Agri automated system in various cropping systems around the world

Pierre Defourny[a], Sophie Bontemps[a,*], Nicolas Bellemans[a], Cosmin Cara[b], Gérard Dedieu[c], Eric Guzzonato[d], Olivier Hagolle[c], Jordi Inglada[c], Laurentiu Nicola[b], Thierry Rabaute[d], Mickael Savinaud[d], Cosmin Udroiu[b], Silvia Valero[c], Agnès Bégué[e,f], Jean-François Dejoux[c], Abderrazak El Harti[g], Jamal Ezzahar[h,n], Nataliia Kussul[i], Kamal Labbassi[j], Valentine Lebourgeois[e,f], Zhang Miao[k], Terrence Newby[l], Adolph Nyamugama[l], Norakhan Salh[m], Andrii Shelestov[i], Vincent Simonneaux[c,n], Pierre Sibiry Traore[o], Souleymane S. Traore[p], Benjamin Koetz[q]

[a] Earth and Life Institute, Université catholique de Louvain, 2 Croix du Sud bte L7.05.16, 1348 Louvain-la-Neuve, Belgium
[b] CS Romania S.A., 29 Strada Pacii, 200692, Craiova, Romania
[c] Centre d'Etudes Spatiales de la BIOsphère CESBIO, Université de Toulouse, CNES/CNRS/IRD/UPS, 18 Avenue Edouard Belin, 31401 Toulouse, France
[d] CS Systèmes d'Information, 5 rue Brindejonc des Moulinais, 31506 Toulouse, France
[e] CIRAD-UMR TETIS, Maison de la télédétection, 500 rue J.-F. Breton, 34093 Montpellier, France
[f] TETIS, Université de Montpellier, CIRAD, Irstea, AgroParisTech, CNRS, Montpellier, France
[g] Faculty of Sciences and Techniques, Sultan Moulay Slimane University, POB 523, Béni Mellal, Morocco
[h] École Nationale des Sciences Appliquées de Safi, Université Cadi Ayyad, 46000 Safi, Morocco
[i] Space Research Institute of National Academy of Sciences of Ukraine and State Space Agency of Ukraine, 40 prosp. Glushkov, build.4/1, 03680 Kyiv, Ukraine
[j] Université Chouaib Doukkali, Morocco
[k] Institute of Remote Sensing and Digital Earth, Chinese Academy of Sciences, Olympic Village Science Park, West Beichen Road, Chaoyang, Beijing 100101, China
[l] Agricultural Research Council (South Africa), Private Bag X79, 0001 Pretoria, South Africa
[m] Ministry of Agriculture, Sudan
[n] Laboratoire Mixte International TREMA, Centre Geber, Faculté des Sciences de Semlalia, 40000 Marrakech, Morocco
[o] International Crops Research Institute for the Semi-Arid Tropics (ICRISAT), Samanko Stn., POB 320, Bamako, Mali
[p] Institut d'Economie Rurale, Bamako, Mali
[q] ESA-ESRIN, European Space Agency, Via Galileo Galilei, Casella Postale 64, 00044 Frascati, Rome, Italy

ARTICLE INFO

ABSTRACT

The convergence of new EO data flows, new methodological developments and cloud computing infrastructure calls for a paradigm shift in operational agriculture monitoring. The Copernicus Sentinel-2 mission providing a systematic 5-day revisit cycle and free data access opens a completely new avenue for near real-time crop specific monitoring at parcel level over large countries. This research investigated the feasibility to propose methods and to develop an open source system able to generate, at national scale, cloud-free composites, dynamic cropland masks, crop type maps and vegetation status indicators suitable for most cropping systems. The so-called Sen2-Agri system automatically ingests and processes Sentinel-2 and Landsat 8 time series in a seamless way to derive these four products, thanks to streamlined processes based on machine learning algorithms and quality controlled *in situ* data. It embeds a set of key principles proposed to address the new challenges arising from countrywide 10 m resolution agriculture monitoring. The full-scale demonstration of this system for three entire countries (Ukraine, Mali, South Africa) and five local sites distributed across the world was a major challenge met successfully despite the availability of only one Sentinel-2 satellite in orbit. *In situ* data were collected for calibration and validation in a timely manner allowing the production of the four Sen2-Agri products over all the demonstration sites. The independent validation of the monthly cropland masks provided for most sites overall accuracy values higher than 90%, and already higher than 80% as early as the mid-season. The crop type maps depicting the 5 main crops for the considered study sites were also successfully validated: overall

accuracy values higher than 80% and F1 Scores of the different crop type classes were most often higher than 0.65. These respective results pave the way for countrywide crop specific monitoring system at parcel level bridging the gap between parcel visits and national scale assessment. These full-scale demonstration results clearly highlight the operational agriculture monitoring capacity of the Sen2-Agri system to exploit in near real-time the observation acquired by the Sentinel-2 mission over very large areas. Scaling this open source system on cloud computing infrastructure becomes instrumental to support market transparency while building national monitoring capacity as requested by the AMIS and GEOGLAM G-20 initiatives.

1. Introduction

For decades, satellite remote sensing was promoted as a key data source for operational agriculture monitoring. The coarse to medium resolution optical instruments on board of SPOT-Vegetation, MODIS and PROBA-V satellites play a major role in operational near real-time crop monitoring thanks to their daily revisit cycle, their global coverage, their long-term archive and their access at no or limited cost. The Landsat satellite series permitted developing operational crop type mapping at high resolution for some specific agricultural landscapes characterized by large fields such as in the United States (Boryan et al., 2011; USDA, 2018; Yan and Roy, 2014) and Canada (McNairn et al., 2009; Fisette et al., 2015; Davidson et al., 2017). However, the 16-day revisit cycle was found problematic for near real-time crop type mapping and in regions with persistent cloud cover due to the limited number of valid observations (Blaes et al., 2005; Johnson, 2014; McNairn et al., 2009; Whitcraft et al., 2015b). Furthermore, the 30-m spatial resolution does not allow resolving the individual fields in many agricultural landscapes, preventing any parcel-based application on most cropping systems around the world. For instance, the advanced crop monitoring system developed over India (Ray et al., 2016) is only possible thanks to a combination of the Indian Resourcesat-2 AWiFS and LISS-IV instruments (*i.e.* spatial resolution of 56 m and 5,8 m respectively). Commercial satellite constellations such as RapidEye allow monitoring agricultural landscapes with a spatial resolution higher than 5 m (Lussem et al., 2016; Xu et al., 2016). However, their small scene footprint combined with rather poor radiometric and atmospheric correction were identified as significant issues preventing operational wall-to-wall consistent coverage over large areas in addition to the cost constraint (Davidson et al., 2017). SPOT 6&7 imagery is similarly used over targeted areas for commercial crop advice programs (*e.g.* FARM-STAR service in France (WWW4)) or specific applications like nitrogen management (*e.g.* MasAgro GreenSat project in Mexico (WWW6)), but cannot be generalized due to their significant cost and still limited scene footprint.

Building on the Landsat and SPOT missions' legacy, the Sentinel-2 (S2) satellite constellation and its MultiSpectral Instrument (MSI) were designed in the framework of the European Copernicus program for land surface and agriculture monitoring to measure the reflected solar spectral reflectance in 13 bands ranging from the visible to the ShortWave Infrared (SWIR) bands. The spectral bands include three narrow bands for cloud screening and atmospheric correction at 60 m, three red-edge bands and two SWIR bands at 20 m providing key information about vegetation, as well as the classical blue, green, red and near infrared bands at 10 m (Gascon et al., 2017). Since late 2015, the Sentinel-2A (S2A) satellite provides a revisit time of 10 days over Europe and Africa and of 20 days elsewhere while the successful launch of Sentinel-2B (S2B) in March 2017 ensures a 5-day revisit time above all landmasses since February 2018. The S2A and S2B space component was designed as a global consistent and long-term solution, whose continuity is ensured beyond at least 2030 with the forthcoming Sentinel-2C and 2D satellites.

Unlike the previous Earth Observation (EO) missions, the wide-swath of S2 combined with its 5-day revisit cycle opened the door for revisiting agricultural mapping and monitoring, and for addressing new challenges, related to the diversity of cropping systems at global scale.

Indeed, the Copernicus open and free access policy coupled with the S2 great image quality performance (Gascon et al., 2017) provides the opportunity to build dense and consistent time series over a growing cycle in most regions of the world. Yet, a key research question concerns the scientific feasibility of a generic exploitation of the S2 time series for agriculture monitoring across the world.

Indeed, up to now, no high spatial resolution agriculture application has been considered beyond national scale for systematic, regular and wall-to-wall monitoring (Fritz et al., 2018). Since decades, comparative analysis of Normalized Difference Vegetation Index (NDVI), Dry Matter Productivity (DMP) or biophysical variables (*e.g.* fraction of Absorbed Photosynthetically Active Radiation (fAPAR) or Leaf Area Index (LAI) time series) derived from 1-km or 250–300 m daily observations has been applied at global scale. Anomaly detection with regard to the last 10 years or profile similarity analysis based on these remotely-sensed biophysical variables are operational for early warning systems in various contexts, for instance the Food and Agriculture Organization of the United Nations (FAO) Global Information and Early Warning System (GIEWS), the Famine Early Warning Systems Network (FEWS-NET) from the United States Agency for International Development (USAID), the Monitoring Agriculture by Remote Sensing (MARS) project of the European Commission Joint Research Centre (JRC), and the CropWatch Program of the Chinese Academy of Sciences. However, these approaches always consider the agricultural landscape in a broad sense (Vancutsem et al., 2012), trying to un-mix natural and cultivated vegetation in the best case (Genovese et al., 2001), but never separately monitoring the different crops in the landscapes.

The diversity of agricultural practices and cropping systems observed around the world has already been highlighted by Biradar et al. (2009). More recently, Waldner et al. (2016) demonstrated that the classification performance is much more dependent on the type of cropping systems, than on the classification method. This result, based on the Joint Experiment for Crop Assessment and Monitoring network (JECAM) (WWW5), relied on the comparison of five different cropland mapping methodologies over five contrasting JECAM sites of medium to large field size, using the same time series of 7-day 250 m Moderate Resolution Imaging Spectroradiometer (MODIS) mean composites.

In this new context, the European Space Agency (ESA) funded the Sentinel-2 for Agriculture (Sen2-Agri) project (WWW3), which aimed at developing an open-source system based on generic time series analysis methods for crop mapping and monitoring, and which could be applied anywhere, taking advantage of the global availability of EO high resolution time series acquired by S2 and Landsat 8 (L8). The scientific challenge was to design an EO exploitation strategy globally applicable and able to ingest time series in a generic and systematic way, in order to make the most of the new EO high resolution acquisition systems. The methodological design of this ambitious strategy follows previous inter-comparison of classification methods of high resolution and frequent EO data available from the SPOT-4 (Take 5) initiative. These benchmark studies were conducted across the JECAM network that provides sites distributed across the world (Inglada et al., 2015; Matton et al., 2015; Valero et al., 2016). The Sen2-Agri open source system design and development addressed the top priority crop monitoring needs in support of the national reporting capacities for the "Sustainable Development Goal 2 – Zero Hunger" (SDG-2) and the GEOGLAM initiative (Whitcraft et al., 2015a, Parihar et al., 2012).

The objective of this paper is to investigate whether the generic time series analysis methods provided by the Sen2-Agri platform can be successfully applied to various cropping systems to deliver key agriculture information in a timely and accurate manner at 10 m resolution over large areas (*i.e.* national scale). The study provides an overview of the methods and algorithms implemented in the Sen2-Agri system, presenting for the first time the underlying innovative ideas specifically designed to high resolution nation-wide agriculture monitoring. Then, the paper reports and discusses the performance of the Sen2-Agri system through local and national scale cases studies over sites spanning a wide range of crops, landscapes and agricultural practices for the agricultural season 2016–2017.

2. Overall approach

2.1. Requirements and challenges for a high-resolution nation-wide agriculture monitoring system

The top priority information required by the stakeholders in charge of crop monitoring has not evolved much since the early days of satellite remote sensing. Again in 2015, several surveys and stakeholder meetings organized at international level defined four basic products expected from the current EO systems (Bontemps et al., 2015): (i) regular cloud-free surface reflectance images at high resolution to distinguish the individual fields; (ii) an early cropland mask allowing the operational early warning systems to focus on the medium resolution NDVI time series analysis on the land actually cultivated; (iii) a crop type map at a spatial resolution compatible with field size to locate the crop distribution and to possibly serve as early area indicator for the main crop groups; (iv) wherever possible, a continuous time series of NDVI and LAI at high resolution to describe the vegetation development on very regular basis.

Any nationwide remote sensing solution aiming to address these agricultural user requirements faces four underestimated challenges largely unresolved for processing high spatial resolution EO time series. First, a significant agro-climatic gradient spanning over the national territory gradually shifts the cropping calendar of most crops, as well as the crop type distribution, making the scaling up to national level rather problematic. Second, overlapping and interweaving growing seasons for a given area makes the concept of an annual cropland mask rather irrelevant as the identification of the start and the end of an agricultural season is very arbitrary or impossible. For instance, in Northern European countries, winter wheat of the next growing season is sowed months before the harvest of spring crops like maize or sugar beet; not to mention the nitrogen fixing and cover crops planted between the main crops or the complexity of multiple growing cycles irrigated all year round. Third, unlike medium resolution daily observations providing consistent 7-day or 10-day composite time series, high spatial resolution EO time series suffer from spatially irregular image density and heterogeneous distribution of observation dates due to the occurrence of clouds, orbit cycle, and overlapping observations, thus increasing the complexity of model calibration and pixel classification. The last and fourth issue is the large discrepancy between cadastral parcels and agriculture management units preventing the use of any up-to-date field boundary layer valid for the ongoing growing season, even in most developed countries. Such an annually updated layer would be instrumental for processing 10 m time series in a much more constrained approach.

2.2. Key principles for a high-resolution automated processing system

As a contribution to properly answer these four unresolved challenges, a combination of innovative elements were developed and implemented in the Sen2-Agri system with the aim to move from data set processing on a yearly basis, to a continuous delivery of information, not only of NDVI or vegetation conditions but also of cropland masks and crop type maps. These developments rely on the following basic ideas.

1. The methods implemented in the Sen2-Agri system should make a maximal use of the EO time series information, and should not rely on single date images nor on seasonal composites.
2. In order to have homogeneous time series, a regular sampling of observations is necessary. Temporally interpolated surface reflectance values (with a time step equivalent to the sensor revisit cycle) could maintain the information content, deal with the spatial heterogeneity of time series density and observation date, and fill the gaps due to clouds or missing values. A high quality cloud mask and atmospheric correction is necessary to get consistent and smooth time series.
3. A monthly updated cropland mask provides dynamic cropland information in order to deal with the overlapping cropping seasons, with possible cropping calendar shifts along agro-climatic gradients, and with asynchronous cropping patterns due to irrigation. The relevant cropland mask corresponding to a given month will be selected to address a specific application.
4. The monthly cropland mask should be produced based on a 12-month rolling period (*i.e.* EO time series corresponding to the last 12 months) to enhance the cropland discrimination accuracy and to cope with the frequent co-occurrence of the growing season and the cloudiest periods.
5. The availability of *in situ* data is key for cropland and crop type mapping. A methodology providing a cropland mask without any *in situ* data is implemented for areas not accessible on the field for various reasons (*e.g.* conflict, flooding). It is based on spectral features calculated at specific stages of the growing cycle rather than for any *a priori* date or any given time interval (more detail in Section 2.4.2). In this way, surface reflectance values are composited based on specific events or typical characteristics of annually cultivated fields (*e.g.* bare soil period, fast growing period, *etc*.), thus addressing the challenge of the agro-climatic gradient.
6. The decoupling between cropland mapping and crop type discrimination corresponds to a hierarchical approach to take advantage of different classification strategies in the absence of pre-existing field boundaries layers like the Land Parcel Information System available in most European countries (JRC, 2001).
7. While the EO data near-real-time processing should be based on tiles to be fully scalable and run in parallel, the machine learning classification models (for both cropland and crop type maps) must be trained over larger areas corresponding to agro-climatic zones rather homogeneous in terms of climate, agro-ecological conditions (relief, soil, *etc*.), cropping systems and agricultural practices. The use of such a stratification avoids requiring a complete set of *in situ* data for each tile and therefore ensures the validity of the trained models over large areas. It also allows coping with agro-climatic gradients inducing a very diversity of crop calendars and growing conditions.
8. The machine-learning algorithm to be selected must be able to cope with the diversity of spectro-temporal signatures for a given crop due to various planting dates, cultivars, and weather conditions, still present in any agro-climatic zone.

All these principles have been embedded in the design of the Sen2-Agri system to deliver a flexible and highly performing tool. While the Sen2-Agri system has been fully documented (ESA Sen2-Agri, 2016) and already found uptake by operational stakeholders, it is the first time that these underlying innovative ideas are consistently explained, as well as applied, validated and discussed through different case studies.

2.3. The Sen2-Agri system

The ESA Sen2-Agri system is an operational standalone processing system made of modules generating agricultural products from S2 L1C and/or L8 L1T time series along the growing season. The use of only S2 or only L8 or combining S2 and L8 time series is a choice offered to the user. These different products consist of:

(i). monthly cloud-free composites of surface reflectance at 10–20 m resolution;

(ii). monthly dynamic cropland masks, delivered from the agricultural mid-season onwards;

(iii). cultivated crop type maps at 10 m resolution for main crop groups, delivered twice during agricultural seasons;

(iv). time series of vegetation status indicators, NDVI and LAI, describing the vegetative development of crops each time a cloud-free observation is recorded.

The Sen2-Agri system is based on machine learning algorithms and relies on *in situ* data to map the cropland and crop type classes (even if a solution to generate cropland mask without any *in situ* data is also provided). The Sen2-Agri system is open-source, allowing any user to generate near real-time products tailored to his needs at its own premises or on cloud computing infrastructure (Fig. 1). It is composed of a set of independent processing modules orchestrated by a data-driven approach. Before generating any product, L1 Top of Atmosphere (TOA) reflectance (S2 L1C and L8 L1T product) is converted to accurate Bottom-Of-Atmosphere (BOA) reflectance, with a good quality cloud mask (L2A product).

The main goal of the system is to enable handling large volumes of EO data in a timely manner and to be easily scaled up to cover the whole region of interest. The Sen2-Agri system has been designed to facilitate the expansion of the hardware or software configuration without redesign and with almost no downtime, being able to support additional processing needs.

The building blocks of the software solution for the modules rely on the Orfeo Toolbox (OTB) (Grizonnet et al., 2017; WWW8), a high-resolution image processing toolbox, open source, portable and able to be extended to complement the suite of the already developed algorithms. These blocks are organized into several processing chains while being coordinated by a custom developed orchestrator which can dispatch the processing jobs to several nodes *via* SLURM, an open source resource manager (https://slurm.schedmd.com/). The level-3 and level-4 processing blocks are fully compatible with the S2 Toolbox (WWW2) and can be integrated in the common Sentinels Application Platform (SNAP) through external tool adapters, thereby allowing their usage either independently or as a processing chain outside the Sen2-Agri system.

2.4. The Sen2-Agri module functionalities

The Sen2-Agri algorithms allowing the generation of each product were selected based on comprehensive benchmarking, described in detail in Bontemps et al. (2015). This benchmarking took place before the S2 era, based on the SPOT 4&5 (Take 5) time series, which mimicked the "Sentinel-2 like conditions" (Hagolle et al., 2013; Hagolle et al., 2015). Inglada et al. (2015), Matton et al. (2015) and Valero et al. (2016) described the respective methods and the benchmarking results. During this research, methods were adjusted to S2 data and fine-tuned to near real-time operational conditions.

All algorithms are designed to run with S2 and/or L8 images that have been atmospherically-corrected using the Multisensor Atmospheric Correction and Cloud-Screening (MACCS) algorithm, included in the Sen2-Agri system.

The specific strength of MACCS is to use multi-temporal criteria to build the various masks (land, water, snow, cloud and cloud shadow) and to detect the aerosols before the atmospheric correction (Hagolle et al., 2008; Hagolle et al., 2010).

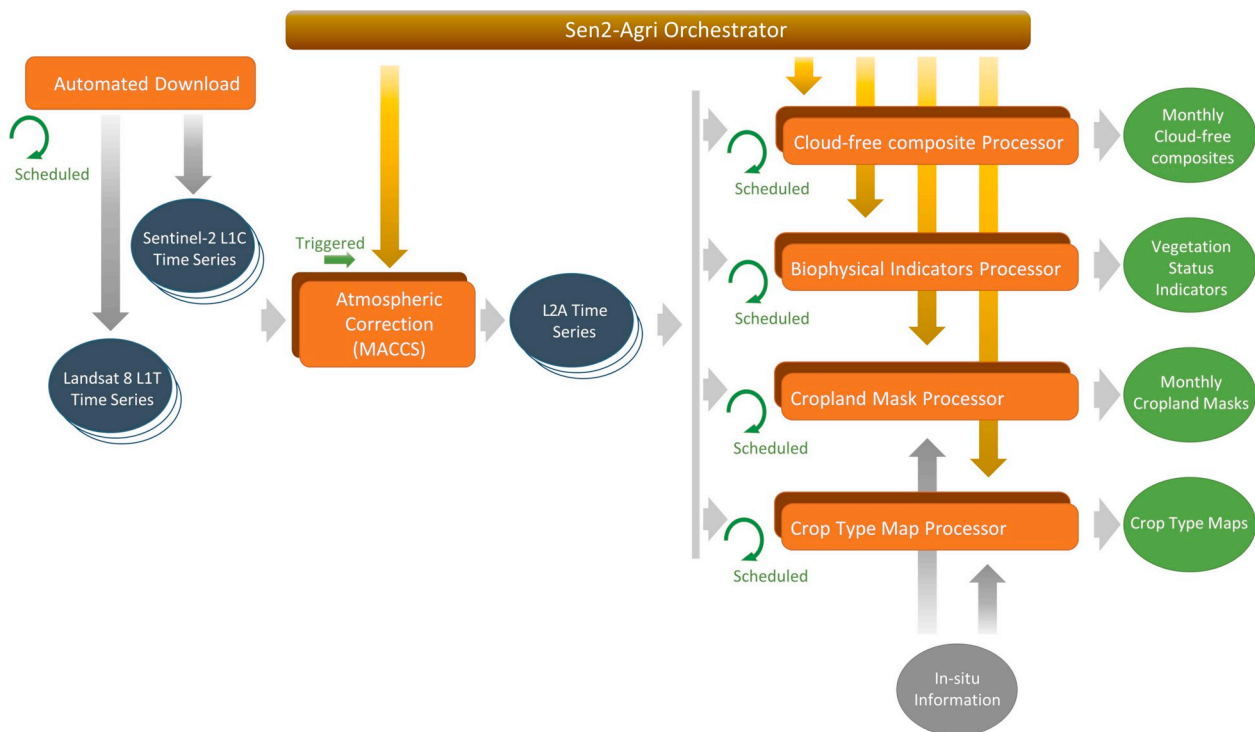MACCS was selected for the high quality of its cloud and cloud

Fig. 1. Diagram of Sen2-Agri processing system made of independent processing modules orchestrated by a data-driven approach, *i.e.* running according to the data flows coming from S2 and L8 catalogs.

shadow mask, which is of critical importance for operational applications. Indeed, the Atmospheric Correction Inter-comparison eXercise (WWW1) pointed out its high performance for water vapour retrieval and showed that MACCS provided accurate and robust surface reflectance estimates for all test sites (Doxani et al., 2018). The only limitations identified during this exercise concern (i) a slightly heavier processing cost than other state-of-the-art atmospheric correction processors due to the basic requirements of the underlying multi-temporal algorithm and (2) some difficulties to retrieve the Aerosol Optical Depth (AOT) when the surface reflectance is high, which corresponds to arid sites and should have a limited impact for agriculture applications.

The methods implemented in each processing module corresponding to the respective product are briefly described in this section.

2.4.1. Monthly composites of surface reflectance

Monthly composites are generated using a weighted average algorithm, which consists in averaging cloud-free surface reflectance values over a given period (Vancutsem et al., 2007a; Vancutsem et al., 2007b). The method relies on the repetitivity of observations to statistically reduce errors that could happen due to undetected clouds or cloud shadows or atmospheric correction errors. For each monthly composite, a compositing period longer than a month is used (50 days) to promote a lower amount of remaining cloudy pixels. The reference date of the composite corresponds to the first day of the month, and the algorithm makes use of the 25 days before and the 25 days after this reference date. L2A images are first pre-processed to remove directional effects, using a model based on Maignan et al. (2004) and Bréon and Vermote (2012). The directional model is Ross-Thick/Li-Sparse-Reciprocal BRDF (Li and Strahler, 1992; Ross, 1981), following the study of Roy et al. (2016). There is no inter-calibration performed between the S2 and L8 sensors. L8 spectral bands are resampled to the spatial resolution of the corresponding S2A spectral bands (10 m for L8 bands 2, 3 and 4 and 20 m for the L8 bands 5, 7 and 8). Neither the blue band nor the 60-m S2A bands are provided in the composite. Averaged observations are weighted pixel wise in a way to favour dates with low aerosol content, low cloudiness and pixels far from clouds (Hagolle et al., 2015). A greater weight is also given to acquisitions closer to the central date and acquired by the S2A sensor.

In order to meet the challenges of near real-time delivery and being able to deliver the monthly composite a few days after the end of the acquisition period, the algorithm has been implemented as a recurrent process. The algorithm is not run once for all acquisitions at the end of the acquisition period, but at each acquisition, generating a first intermediate composite from the first image and updating it each time a new image is available. These intermediate products are not delivered by the system. The overall process is illustrated in Fig. 2. The algorithm is applied over all pixels identified as "Land" or "Water" by the MACCS algorithm. "Snow", "Cloud" and "Cloud shadow" pixels are added at the end of the process if no "Land" or "Water" pixel has been observed during the acquisition period.

2.4.2. Monthly cropland masks

While the class "cropland" has no clear definition in the literature, the research relies on the "cropland" definition proposed by the JECAM network in the framework of GEOGLAM: the "*annual cropland from a remote sensing perspective is a piece of land of a minimum 0.25 ha (minimum width of 30 m) that is sowed/planted and harvestable at least once within the 12 months after the sowing/planting date. The annual cropland produces an herbaceous cover and is sometimes combined with some tree or woody vegetation*" (JECAM, 2018). In this definition, perennial crops and fallows are excluded from the cropland class. There are three further important considerations to this definition: 1) sugarcane plantations and cassava crops are included in the cropland class even though they may have a longer vegetation cycle than 12 months and are not planted yearly; 2) small fields taken individually, such as legumes, do not meet the minimum size criteria of the cropland definition; 3)

greenhouse crops cannot be monitored by satellite remote sensing and are thus excluded from the definition.

The developed method to map the cropland class starts from the original L2A time series (not from the above-mentioned composites), fills the data gaps and relies on a supervised Random Forest (RF) algorithm. Two options are implemented to build the RF model depending on the availability or not of *in situ* data (Fig. 3).

The first option assumes the availability of *in situ* data, corresponding to (i) a set of crop type samples characterizing the diversity of the cropland class and (ii) a set of non-cropland samples corresponding to the main other land cover classes (vegetation, water, bare soil, *etc.*). In this case, the RF model is built on statistical and temporal features for each crop type. Temporal features are derived from the NDVI time series while statistical features are extracted from Normalized Difference Water Index (NDWI), brightness (defined as the Euclidean norm of the surface reflectance values in green ($\rho_{0.560}$), red ($\rho_{0.665}$), NIR ($\rho_{0.842}$) and SWIR ($\rho_{1.610}$)) and S2 red-edge indices. The S2 red-edge indices are as follows (with ρ being the reflectance value in a spectral channel given by its central wavelength) (Hatfield and Prueger, 2010):

Red edge NDVI = $(\rho_{0.842} - \rho_{0.740})/(\rho_{0.842} + \rho_{0.740})$ (Gitelson and Merzlyak, 1994)

S2 Red Edge Position = $705 + 35 \times (0.5 \times (\rho_{0.783} + \rho_{0.665}) - \rho_{0.705})/(\rho_{0.740} - \rho_{0.705})$

Plant Senescence Reflectance Index (PSRI) = $(\rho_{0.665} - \rho_{0.490})/\rho_{0.705}$ (Merzlyak et al., 1999)

Chlorophyll Red − Edge = $\rho_{0.705}/\rho_{0.842}$

The reader is referred to Valero et al. (2016) to get a detailed description of the whole set of features.

Since the NDVI temporal features are calculated for all dates of the time series, it is critical to get the same dates on the whole area of interest, independently from the sensor orbits. A temporal resampling is therefore implemented along with the gap filling, at a sampling rate corresponding to the sensor revisit cycle.

In the second option, in the absence of any *in situ* data, calibration data are selected from an existing reference map (*i.e.* a general land cover map at local, regional or global scale) and cleaned using an iterative trimming process (Desclée et al., 2006; Radoux et al., 2014) before being used by the RF algorithm. The by-default reference map currently available in the Sen2-Agri system is the ESA Climate Change Initiative (CCI) global Land Cover Map from 2010 (Land Cover CCI Product User Guide, 2017), but the users have the possibility to upload their own map if preferred.

Land cover maps often do not provide crop type information and it is important to define features as generic as possible in order to be independent of the crop growing calendar and to allow dealing with the cropland diversity and the gradient across landscape. In this case, the RF model is built based on temporal features corresponding to specific stages of the growing cycle: (i) the date of the maximum and minimum NDVI slopes, (ii) the date of the maximum and minimum NDVI values, and (iii) the date of the maximum red band value (Matton et al., 2015; Lambert et al., 2016). The gap filling step is coupled with a smoothing
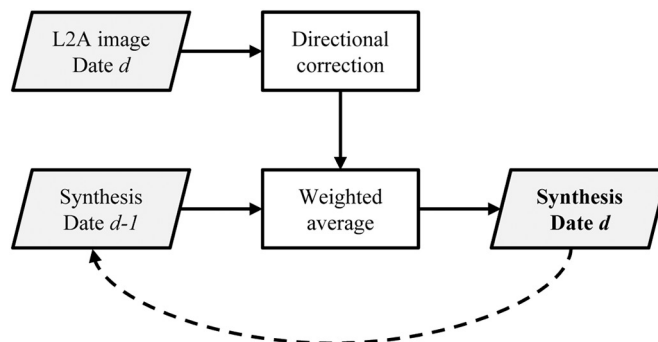
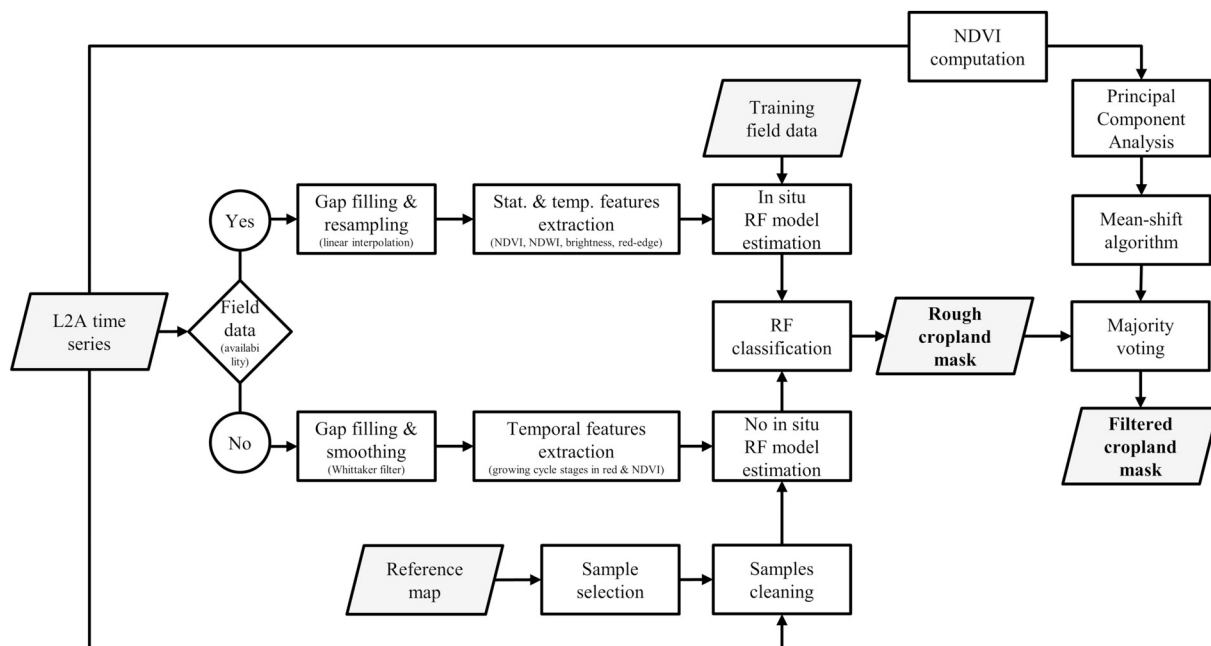**Fig. 2.** Workflow of the weighted average compositing process.

Fig. 3. Workflow of the method developed to generate the cropland mask for each agro-climatic stratum separately.

using a Whittaker filter, to make possible the robust extraction of these temporal metrics.

In the case users select both S2A and L8 sensors, their respective L2A surface reflectance time series are pre-processed independently. S2A and L8 L2A time series are then concatenated, providing to the RF algorithm a mixed S2A and L8 cloud-free time series.

In both options, with and without *in situ* data, an *a posteriori* optional step allows filtering the cropland mask, using majority voting over objects delineated by a mean-shift algorithm, applied on the outcome of a Principal Component Analysis of NDVI time series (Valero et al., 2016).

For large-scale monitoring, the Sen2-Agri system also allows the user to define a stratification of the considered region into independent sub-regions or strata which are assumed to be homogeneous regarding climate and agro-ecological conditions (relief, soil, *etc.*) as well as agricultural practices. All *in situ* samples (coming either from field data or from the reference map) within a stratum are considered to build a stratum-specific RF model, which is then applied to all tiles belonging to this stratum. Such stratification is to be defined by the user.

The proposed algorithm makes full use of the S2A high observation frequency by relying on temporal features. It is therefore recommended

to wait for the mid-season to get meaningful temporal features and thus, a more satisfactory result.

2.4.3. Cultivated crop type maps

L2A surface reflectance time series are interpreted into a crop type map, based on supervised learning with RF or Support Vector Machine (SVM) classifiers (Fig. 4). The experience carried out in the benchmarking (Inglada et al., 2015) showed that RF performs generally better, but SVM is expected to provide better classification results in the specific case of classes with few calibration samples. RF is therefore the by-default classifier in the Sen2-Agri system.

The method requires the availability of *in situ* data.

Linear interpolation and gap filling of surface reflectance time series are first applied like for the cropland mask based on *in situ* data. These two steps are applied independently for S2 and L8 time series which are then concatenated before feeding the RF or SVM classifier. Features extracted for the classification are surface reflectance values in the S2 bands 3 ($\rho_{0.560}$), 4 ($\rho_{0.665}$), 5 ($\rho_{0.705}$), 6 ($\rho_{0.740}$), 7 ($\rho_{0.783}$), 8 ($\rho_{0.842}$), 11 ($\rho_{1.610}$) and 12 ($\rho_{2.190}$), NDVI, NDWI and brightness (defined as the Euclidean norm of the surface reflectance values in green ($\rho_{0.560}$), red ($\rho_{0.665}$), NIR ($\rho_{0.842}$) and SWIR ($\rho_{1.610}$)) calculated for each date of the
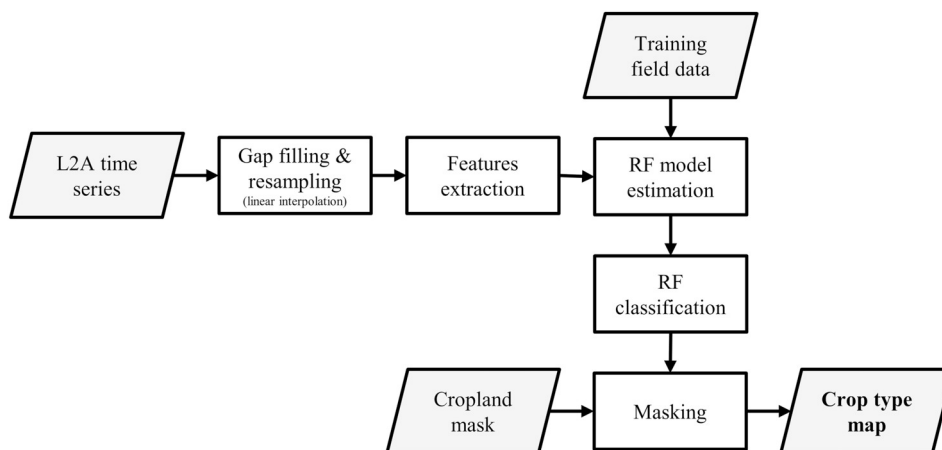

Fig. 4. Workflow of the method developed to generate the crop type map for each agro-climatic stratum separately.

resampled and gap-filled time series. These features and the crop type *in situ* data are then used to train the RF or SVM classifier and generate the crop type map. The reader is referred to Inglada et al. (2015) for a complete description of the method.

Like for the cropland mask, in the case of large regions of interest, the user is invited to provide a stratification to allow the classifier being learned for each individual stratum. The diversity of crop conditions is clearly related to the different cropping systems, the variability of associated crop management, and the impact of agro-climatic conditions interacting with the soil properties and the agricultural practices.

2.4.4. Vegetation status maps based on NDVI and LAI

The vegetation status product consists in NDVI and LAI maps generated for each S2 or L8 acquisition. S2A and L8 sensors are processed independently, resulting in distinct NDVI and LAI time series for each sensor. NDVI computation relies on the S2 band 8 and not 8a, thus being resampled at 10 m. The difference between S2 and L8 bands and the absence of intercalibration between sensors prevent the use of any quantitative combination of both NDVI time series. On the other hand, LAI retrieval is performed using a non-linear regression model established separately for S2 and for L8. The well-known BV-NET approach developed and validated by Weiss et al. (2002) allows computing the regression model based on satellite surface reflectance values simulated using the ProSail model (Feret et al., 2008; Jacquemoud et al., 2009). Fig. 5 illustrates this LAI retrieval process.

Besides, the Sen2-Agri system proposes two reprocessing options of the single-date LAI products in order to take benefit of the multi-temporal information in the LAI estimation (Fig. 6). First, a near real-time algorithm allows adjusting the LAI estimate based on the two previous acquisitions, weighting them using the LAI retrieval error estimation. The second reprocessing option applicable at the end of the season smooths all the retrieved LAI values by fitting a semi-mechanistic phenological model, *i.e.* the Canopy Structure Dynamic Model (CSDM) (Koetz et al., 2005).

2.5. Strategy for in situ data collection and accuracy assessment

In situ data are mandatory to generate the crop type map and desired for the cropland mask. The two main purposes of *in situ* data collection are the classifier calibration and the output validation.

For the cases studies, the campaigns for *in situ* data collection were distributed over the entire area of interest, whether it was a local site or a full country (more information in Section 3.1). The data were then randomly split into calibration (75%) and validation (25%) sets. These splits were done at the field level (*i.e.* polygons) and not on individual pixels, to ensure the independency of the validation samples. In order to encompass the cropping diversity and the agro-climatic gradients observed over large areas, the national territories were stratified into few strata according to agro-climatic gradients and the corresponding agro-ecosystem types, crop type distributions, and cropping calendars.

A two-stage sampling strategy was applied to ensure a large distribution of the samples and a random component in the sample selection. First, the random selection of Primary Sampling Units delineated by ancillary data (typically, administrative regions) were distributed in the different strata according to their cropland area reported in existing agricultural statistics (*e.g.* FAOSTAT portal (WWW7)) (cropland area-weighted sampling probability). Then, within each Primary Sampling Unit, the sampling proceeds as a "windshield survey" identifying Elementary Sampling Units (minimum 1 ha) along the roads as described in the JECAM guidelines (JECAM, 2018). It is worth mentioning that in the case of cropland mapping, the calibration dataset should encompass the diversity of all land cover types as well.

The validation must provide statistically sound estimates of the overall products accuracy based on independent reference data sets collected during the course of the season. The number of samples, the sampling design, the response design, and the reliability of the data source define the quality of the accuracy estimate. While the *in situ* data are collected as polygons, the accuracy assessment is performed at the pixel-level, over pixels selected randomly amongst all pixels belonging to the polygons specifically set aside for the validation.

Two different metrics based on the confusion matrices were selected to evaluate the performances of the cropland masks and crop type maps. First, the Overall Accuracy (OA) quantifies the overall agreement between the map and the reference information. It is calculated as the total number of correctly classified pixels divided by the total number of pixels:

$$OA = \left(\frac{\sum_{i=1}^{r} n_{ii}}{\sum_{i=1}^{r} \sum_{j=1}^{r} n_{ij}} \right) * 100$$

(1)

with n being the number of pixels and r the number of classes.

Second, the F-Score for the class i (also known as F-1 score or F-measure) measures the accuracy of a class combining the User Accuracy
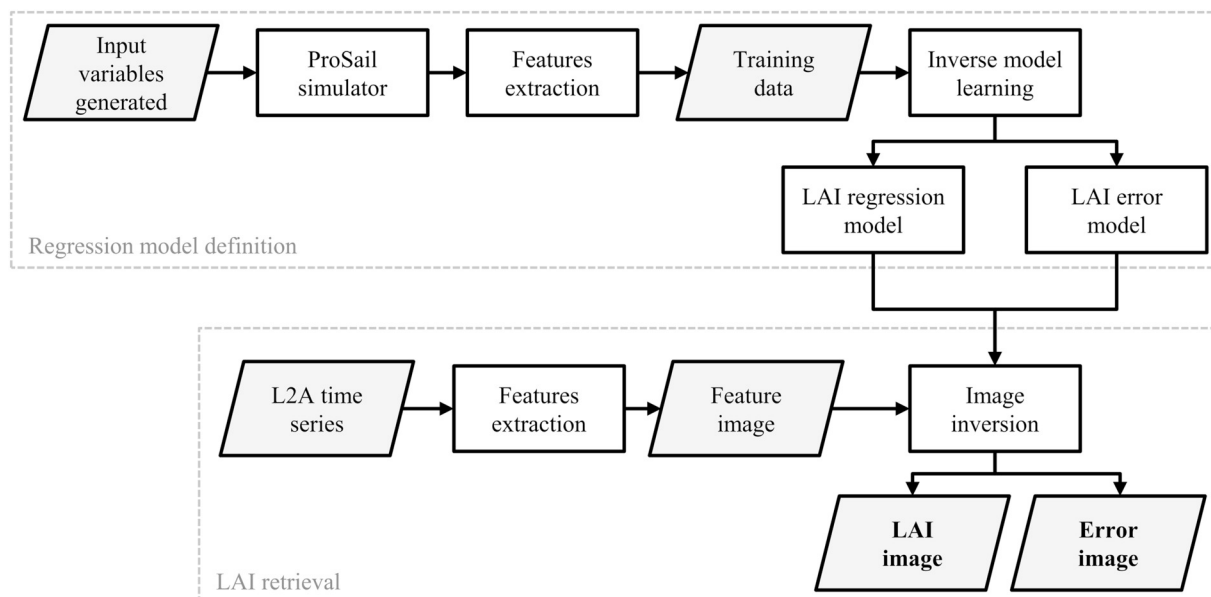

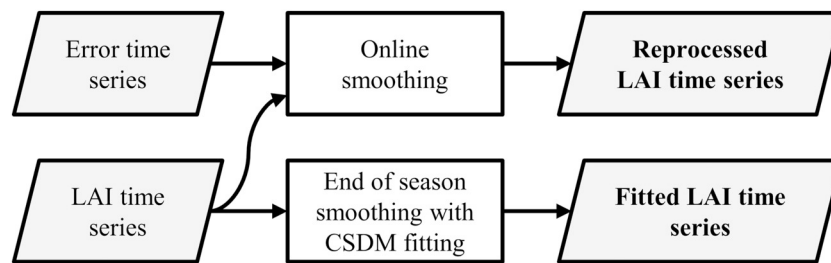**Fig. 5.** Workflow of the method used to retrieve single-date LAI.

Fig. 6. Workflow of the methods developed to generate reprocessed and fitted LAI based on single-date LAI.

(UA or Precision) and Producer Accuracy (PA or Recall) measures. It is calculated as the harmonic mean of the UA and PA and reaches its best value at 1 and worst score at 0:

$$F - Score = 2 \times \frac{UA_i \times PA_i}{UA_i + PA_i} \qquad (2)$$

UA for class i is the fraction of correctly classified pixels regarding all pixels classified as class i in the output:

$$UA_i = \sum_{j=1}^{r} \frac{n_{ii}}{n_{ij}} \qquad (3)$$

PA for class i is the fraction of correctly classified pixels regarding all pixels identified as class i in the reference data:

$$PA_i = \sum_{j=1}^{r} \frac{n_{ii}}{n_{ji}}$$

3. Study areas and available datasets

3.1. Study area

The performances of the Sen2-Agri system were demonstrated through eight local and national scale experiences spanning a wide range of crops, landscapes and agricultural practices. These demonstrations were carried out from February 2016 to June 2017, thus making the full exploitation of the first satellite of the S2 mission. Three nationwide demonstration exercises, respectively in Ukraine, Mali and South Africa, were successfully completed including nationwide *in situ* data collection and production of the respective Sen2-Agri products, then submitted to national stakeholders in the context of three national workshops for assessment and discussion. The Sen2-Agri system has

also been run over five 300 × 300 km sites distributed all over the world (Fig. 7). The diversity of the cropping systems and conditions of observations was well covered by these sites as described in Table 1. For each site, the main crops were identified with the national or local partners, as well as the dates of the monitoring period. In particular, the mid-season date was defined, on a case-by-case basis, to reflect the key moment where early information is useful while ensuring a minimum of 2 months after the start of the season.

3.2. In situ dataset

In situ data were collected in each of the study sites. Thanks to a collaborative effort led by the respective national or local partners, spatial polygons indicating the crop presence and the crop type were obtained from field observations during the main growing season. In Mali and South-Africa, *in situ* data were provided by regular national agriculture statistical surveys, then quality-controlled and harmonized. Samples for non-agricultural land cover classes were obtained by visual interpretation of very high spatial resolution imagery available on line (*e.g.* Google Earth® or Bing Map®) regularly cross-checking with recent S2 cloud-free images. Table 2 characterizes the cropland and non-cropland samples. The distribution of the different land cover classes covered by the cropland and non-cropland samples are provided in Fig. S1 (Supplementary Materials), as well as the crop type classes distribution within the cropland sample.

In Ukraine and Madagascar, *in situ* data were collected through two successive campaigns, at the middle and at the end of the season. Over the other sites, a single dataset was collected and delivered at the end of the growing season.
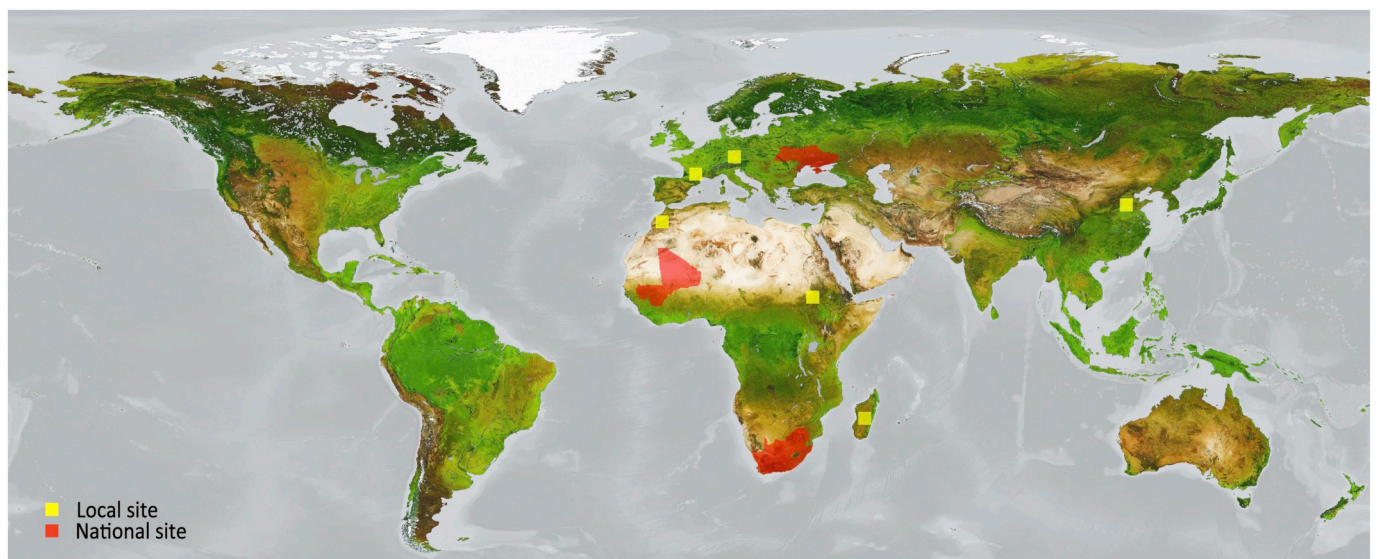

Fig. 7. Distribution of the 8 sites selected for the Sen2-Agri system demonstration. Triangular shapes correspond to local sites, square shapes to the national sites.

Table 1
Main characteristics of the 8 demonstration sites.

Site name and localization	Site area [km²]	Main crops	Field size [ha]	Main growing season		
				Start	Middle	End
China, Shandong	90,000	Maize (92%), vegetables (5%)	0.2–0.8	01/06/2016	01/09/2016	15/10/2016
France, Occitanie	90,000	Maize (43%), wheat (30%), sunflower (14%), rapeseed (6.5%)	10	30/01/2016	31/05/2016	30/11/2016
Madagascar, Antsirabe	90,000	Soybean (38%), maize (27%), paddy rice (23.5%), cassava (11.5%)	0.03	01/10/2016	31/02/2017	15/06/2017
Morocco, Tensift	90,000	Wheat (83%), wheat-oat (11%)	0.5–40	15/01/2016	30/04/2016	31/07/2016
Sudan, White Nile/South-Sudan	90,000	Sorghum (57%), wheat (39%), millet (4%), sesame	1–50	01/07/2016	01/09/2016	15/11/2016
Mali	447,948	Millet (29%), sorghum (20%), maize (13%), paddy rice (11%), cotton (9%)	1–5	01/04/2016	01/09/2016	15/11/2016
Ukraine	576,604	Wheat (24%), sunflower (21%), maize (19%), barley (12%), soybean (7%)	30–250	01/04/2016	01/09/2016	31/10/2016
South Africa – Winter Grain Region (WGR)	619,606	Wheat (33%), fodder crops (45%), oilseed crop (9%), barley (7%)	40	01/05/2016	01/08/2016	15/12/2016
South Africa – Summer Grain Region (SGR)		Maize (55%), fodder crop (23%), sunflower (11%), soybean (8%)	40	15/10/2016	31/01/2017	30/04/2017

3.3. Agro-ecological stratification

Stratifications were defined over Mali, Ukraine, South Africa and Morocco. In Mali, the stratification was designed using the Projet d'Inventaire des Ressources Terrestres (1986), which is recognized as the most reliable pre-existing agro-ecological stratification at the country-scale. Five agro-ecological strata were defined from the original dataset for the cropland and crop type classification. The stratification used in Ukraine is aligned with the four agro-ecological strata commonly used to describe the country (Bogovin, 2001): "Polissia" in the north which is composed by a mixed of natural vegetation, pastures, hayfields and cultivated land, "Forest Steppe" in the country centre, presenting very favourable conditions for agriculture (good moisture conditions and fertile soils), "Steppe" in the south-east also intensively composed of agricultural land, and "Mountains" located in the extreme south-west presenting a low percentage of cultivated land. In Morocco, the stratification was defined manually to separate the Tensift and the Oum Er-Rabia watersheds. In South Africa, the stratification merely corresponds to the Winter Grain Region (WGR) and Summer Grain Region (SGR) since they are geographically separate.

3.4. Satellite time series

All existing S2 L1C and L8 L1T acquisitions covering the spatial extent of the sites and the temporal window of the growing season were automatically downloaded from the ESA Sci-Hub (https://scihub.copernicus.eu/) and United States Geological Survey (USGS) (https://landsat.usgs.gov/) servers by the Sen2-Agri system.

The atmospheric correction and the cloud screening produced surface reflectance values and snow, water cloud and cloud-shadow masks using the MACCS algorithm for all available images with less than 90% cloud cover at the tile or scene level.

The S2A acquisition plan first followed the ramp-up phase with an observation frequency gradually increased, starting from Europe and Africa. As a result, the 10-day observation cycle was available over the European and African demonstration sites, while the Chinese one was first covered every 20 days and then by three out of the four nominal images in autumn 2016. No S2B data was included as the study was completed before the end of the commissioning phase of this second satellite. As examples, the amount of S2 and L8 images processed over the national demonstration sites are described here below. The time series quality is also shortly described. The spatial distribution of the cloud-free observations during the growing season in the S2 and L8 time series is illustrated for each site in Fig. S2 (Supplementary Materials).

For Mali, the L2A surface reflectance time series is made of 1793 S2A tiles (6.27TB) and 477 L8 scenes (0.81TB). The density of the EO times series is generally good and reasonably well distributed along the growing season (Fig. 8(b) and (c)) except in the South-West of the country (Fig. 8(a)).

For Ukraine, the L2A time series is made of 3006 S2A tiles (10.52TB) and 558 L8 scenes (0.99TB). Due to its latitude, Ukraine takes advantage of a large orbit overlap for both S2A and L8 satellites. More than 78% of the Ukraine territory is covered by two L8 orbits in a 16-day Landsat cycle. The quality of the EO time series is generally good with around 20 cloud-free observations per pixel over the season. However, a high heterogeneity in the number of observations can be observed especially along the strips where satellite orbits don't overlap each other.

For South-Africa Winter Grain Region (WGR), the L2A time series is made of 970 S2A tiles (3.39TB) and 183 L8 scenes (0.32TB). The quality of the EO time series is very good. The cloud-free observations are abundant and very well distributed along the growing season. For South-Africa Summer Grain Region (SGR), the L2A time series is made

Table 2
Description of the *in situ* datasets in terms of number of samples and total area covered by the samples.

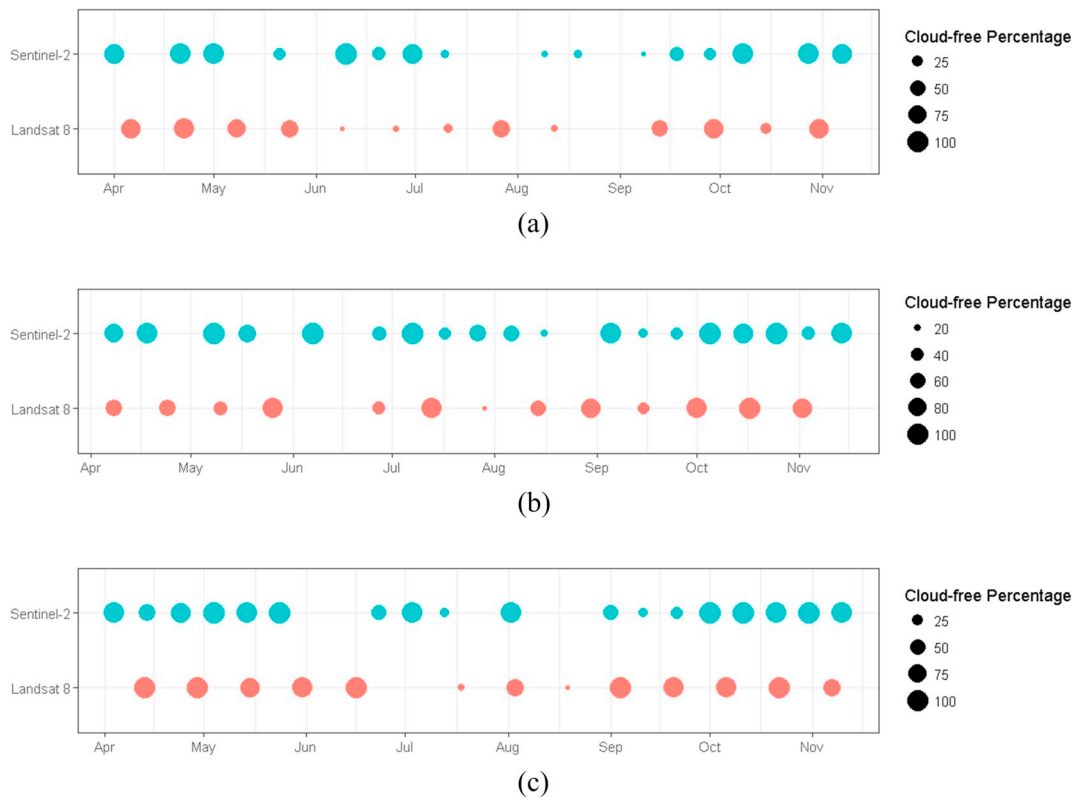| Site	Cropland samples [n/ha]	Non-cropland samples [n/ha]	Spatial distribution
China, Shandong	224/1109	80/1335	Entire site
France, Occitanie	2097/7236	2717/4636	Entire site
Madagascar, Antsirabe	1063/545	545/4045	Focus on Antsirabe JECAM site
Morocco, Tensift	386/1240	589/45,146	Entire site
Sudan, White Nile/South-Sudan	381/10,963	413/1766	No cropland sample in Northern Kordufan and South-Sudan
Mali	5600/6924	2695/36,143	Entire site, spread over 5 strata
Ukraine	5701/100,799	1977/21,068	Entire site, spread over 5 strata
South Africa – WGR	7414/191,169	4801/77,197	Entire site (no stratification)
South Africa – SGR	9194/350,588	4375/100,604	Entire site (no stratification)

Fig. 8. Overview of the S2 and L8 EO data availability in Mali, with details of the cloud-free images distribution along the season and cloud-free percentage for (a) Bougouni - S2 tile 29PPN, (b) Mopti region - S2 tile 30PUA and (c) Nioro du Sahel – S2 tile 29PMS.
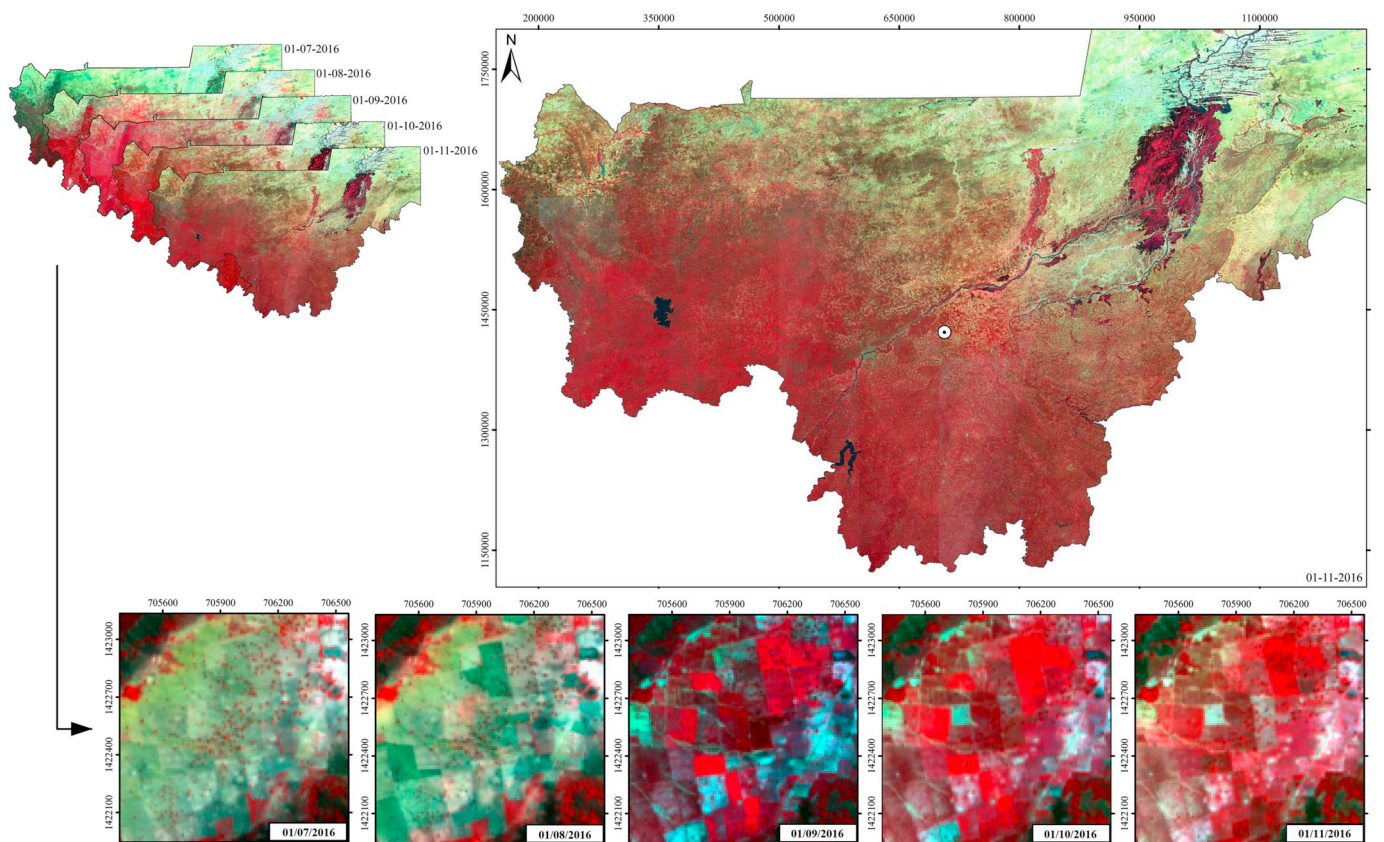

Fig. 9. Series of monthly cloud-free reflectance composites at 10 m resolution along the 2016 growing season over Mali and for a zoom (1:25.000) illustrating the dynamics of local agricultural patterns. UTM coordinates are expressed in meters.

of 2605 S2A tiles (9.12TB) and 678 L8 scenes (1.2TB). The quality of the EO time series is generally moderate with around 13 cloud-free observations per pixel and the density of the time series is drastically decreasing from west to east.

4. Sen2-Agri product assessment

The suite of Sen2-Agri products obtained over the eight study sites, except the composites and the LAI maps, which are not locally trained, were quantitatively assessed based on *in situ* data. For the sake of conciseness, the results analysis does not detail all products over all sites but focuses on the most relevant results to allow assessing Sen2-Agri system performances and its capacity to be relevant for crop monitoring in very different cropping systems.

4.1. Cloud-free surface reflectance composites

Cloud-free surface reflectance composites were generated on a monthly basis during the growing season over all sites except the Chinese one where the revisit frequency was too irregular due to the ramp-up phase. Every monthly composite was produced from a 50-day period in two versions, using S2A data only, and combining both S2A and L8 acquisitions, with the exception of Ukraine where the L8 added value was not assessed for the months of May and June 2016. Fig. 9 shows the composite time series obtained over Mali from July to November 2016. It illustrates the capacity to provide spatially-consistent cloud-free multispectral composites at 10 m resolution over a country like Mali, characterized by significant cloud cover during the growing season. It also shows how this 10 m resolution enables the discrimination of individual fields even in a Sudano-Sahelian context with highly heterogeneous crops growing conditions.

The same kind of series was obtained over all sites, with varying proportions of artefacts and remaining clouds, depending on the conditions of observation. Table 3 quantifies the remaining gaps (clouds and cloud shadows) in terms of pixel proportion in each generated composite, showing both the challenging regions for optical observations and the useful contribution of L8 acquisitions. It allows identifying the sites where the availability of cloud-free observations from S2A and L8 can be critical, as for instance in Mali, South Africa – SGR and

Madagascar. It is worth mentioning that the system is designed to use L8, S2A and S2B imagery, but that in our experiment, only L8 and S2A were available, which is not the case anymore, starting from July 2017.

4.2. Monthly cropland masks

Cropland masks were generated, using both S2A and L8 time series, over all the sites starting from the middle of the season and then monthly updated until the end of season. Fig. 10 shows the cropland mask obtained over Mali at the end of season (November 2016) as the very first 10 m mapping product for this country ever delivered.

For the 3 national demonstration sites, Table 4 reports very high values for the accuracy metrics (*i.e.* OA and F1-Score for cropland and non-cropland classes) computed for cropland masks delivered at the end of season. These OA estimates reaching very high standards reflect the unique density and quality of the EO time series and the performances of the proposed methods. These results are also related to the spatial distribution and the quality of *in situ* data used for calibration. The lower performances observed in South-Africa are clearly due to a poor regional stratification (differentiating only between WGR and SGR), mixing agro-climatic conditions that were too different in landscapes with extensive grasslands. It is also explained by some remaining mismatches between the Sen2-Agri and the national crop nomenclatures. Last but not least, the high accuracy estimates were also enabled by the good matching of the 10-m spatial resolution with cropland patterns, which significantly reduces the proportion of ambiguous mixed pixels.

The accuracy evolution of cropland masks generated with *in situ* data along the season is presented in Fig. 11, over four 300 × 300 km sites located in France, Madagascar, Morocco and Sudan. The accuracy metrics at the end of the season are rather similar to the ones obtained for the national demonstration sites (Table 4). For all sites except Sudan, high accuracy values are obtained right at the middle of the season (the corresponding date being defined for each site in Table 1) and a saturation plateau is reached as early as one or two months after the mid-season. The additional observations acquired later do not improve the accuracy figures until the end of the growing season. These results clearly demonstrate the feasibility to deliver accurate cropland masks as early as the mid-season, independently to the complexity of

Table 3
Missing cloud-free observation (in %) due to clouds or cloud shadows in the monthly reflectance composites during which crops were visible on the ground for the sites (except the Chinese site because of the 20-day revisit cycle). From green to red color to highlight the nearly cloud-free composites (no missing values) to very cloudy ones and the effective contribution of L8 to complement S2 time series.

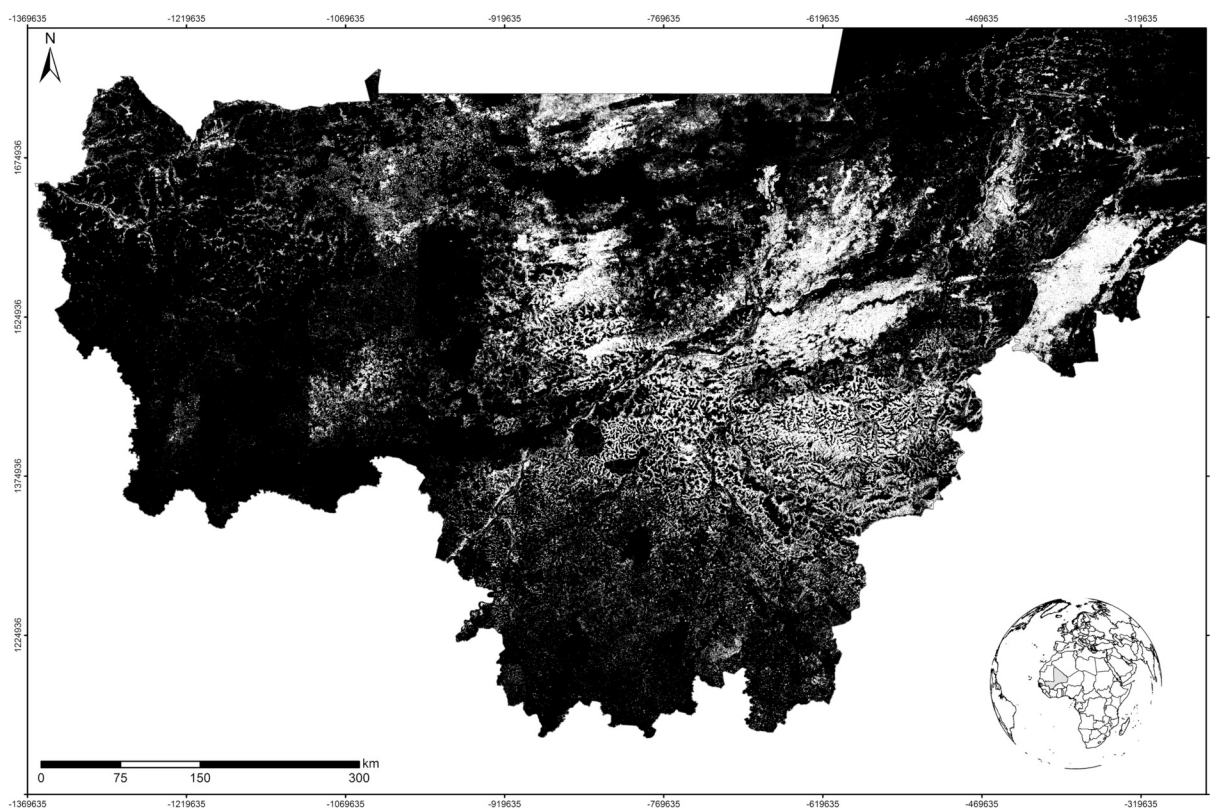| Site	Sensor	Jan	Feb	Mar	Apr	May	June	July	Aug	Sept	Oct	Nov	Dec	Jan	Fev	Mar	Apr	May
								2016								2017		
Morocco	S2 + L8		0.1	0.7	0.5	0.1	0	0										
	S2		11	7.1	0.7	0.7	0.1	0.1										
France	S2 + L8				0.5	1.6	4.9	0.1	0	0.1	0.1							
	S2				3.6	6.3	12.6	0.8	1.1	11.8	1							
South Africa – WGR	S2 + L8						0	3.5	0	0	0.4	0	0.5					
	S2						0.8	7	0.1	0.3	2.7	0.1	0.6					
Ukraine	S2 + L8								0	0	0.9							
	S2						14.5	2.6	1.3	1.1	11.1							
Mali	S2 + L8							1.9	11.2	6.2	0.4	0.1						
	S2							11.6	24.5	18.6	2	0.2						
Sudan	S2 + L8								0.6	0.2	0	0	0.1					
	S2								12.6	2.4	0.2	0.1	0.1					
South Africa – SGR	S2 + L8											1.5	2.4	1.2	3.8	6.9	5.3	
	S2											7.7	11	4.7	9.7	7.4	5.4	
Madagascar	S2 + L8											0.1	2.2	11.4	0.9	28.4	39.8	50.8
	S2											1	5.3	15.7	19.5	35.6	39.7	50.7

Fig. 10. National 10 m cropland mask over Mali for 2016, obtained at the end of the season using S2 and L8 data. White and black represent cropland and non-cropland classes respectively.

Table 4
F1-Scores and OA achieved by the end-of-season cropland mask over three national territories.

Site	F1 cropland	F1 non-cropland	OA [%]
Mali	0.8	0.97	94
Ukraine	0.99	0.94	98
South Africa – WGR	0.88	0.78	85
South Africa – SGR	0.88	0.70	83

the cropping systems.

Finally, the cropland masks produced by the classification method running without any *in situ* data and using the by-default ESA CCI global Land Cover Map from 2010 reference map, were assessed over Ukraine, France, Sudan and China based on the whole *in situ* data set. In Sudan, a second cropland mask was generated using a local Land Cover database generated from 20-m SPOT and 30-m Landsat data in 2011. In spite of the fully autonomous nature of this method and the 300-m resolution of the ESA CCI land cover map, high accuracy results were obtained for most of the sites as shown in Table 5. In all sites, except Sudan, the 300-m ESA CCI land cover map proved to be enough to allow getting a cropland mask with an OA higher than 80% and F1-Score for cropland and non-cropland classes higher than 0.75. In Sudan, the F1-Score for the non-cropland class could be increased from 0.49 to 0.57 using the local database at higher spatial resolution.

Illustrations of the cropland masks generated without *in situ* data over the Chinese, Shandong local site and Ukraine national site are provided in Fig. S3 (Supplementary Materials).

4.3. Crop type maps

Crop type maps were generated for all sites, except for China and Mali, at the middle and at the end of the growing season, from the combined S2 and L8 time series. This production strongly depends on the availability and the quality of *in situ* crop type information available in a timely manner for the calibration. This experience highlights the critical importance of the quality control process regarding the data collected *in situ*. In Mali, the official statistical survey was expected to provide relevant field information about crop type but it finally emerged that the dataset contained significant geolocalization errors, which did not affect the data relevance at the village-level, but certainly prevented from using it for crop type mapping. Because of the S2 operations ramp up phase, the time series acquired over the Chinese site was not dense enough to produce a crop type classification for the season.

For each site, the legend includes the five main crop types or crop groups, as defined by the teams working on the field and in charge of the *in situ* data collection. As an example, Fig. 12 shows the crop type map obtained at the end of the season in South Africa – WGR. The legend includes "winter wheat", "fodder crops", "oilseed crops", "barley" and a fifth class of "other crops". Obviously, the very challenging discrimination between cereals like winter wheat and winter barley is driven only by the difference in crop calendar and leads to a poorer accuracy performance in Ukraine (Table 6). In South Africa, this plant similarity between winter wheat and winter barley also impacts to a lesser extent the discrimination performance. In both countries, winter barley is mostly classified as winter wheat (omission error). This is not so visible through the winter barley F1 Score given the predominance of this crop in the region.

Table 7 focuses on the crop type maps accuracy assessment over the four local sites of France, Morocco, Sudan and Madagascar. It also distinguishes between the crop type maps generated at middle and end of the season. Looking at the end-of-season products, the same kind of conclusions can be drawn here as for the national products: with the exception of Madagascar, OA values are higher than 80% and the F1-Score of the different crop types range between 0.6 and 0.98 with the
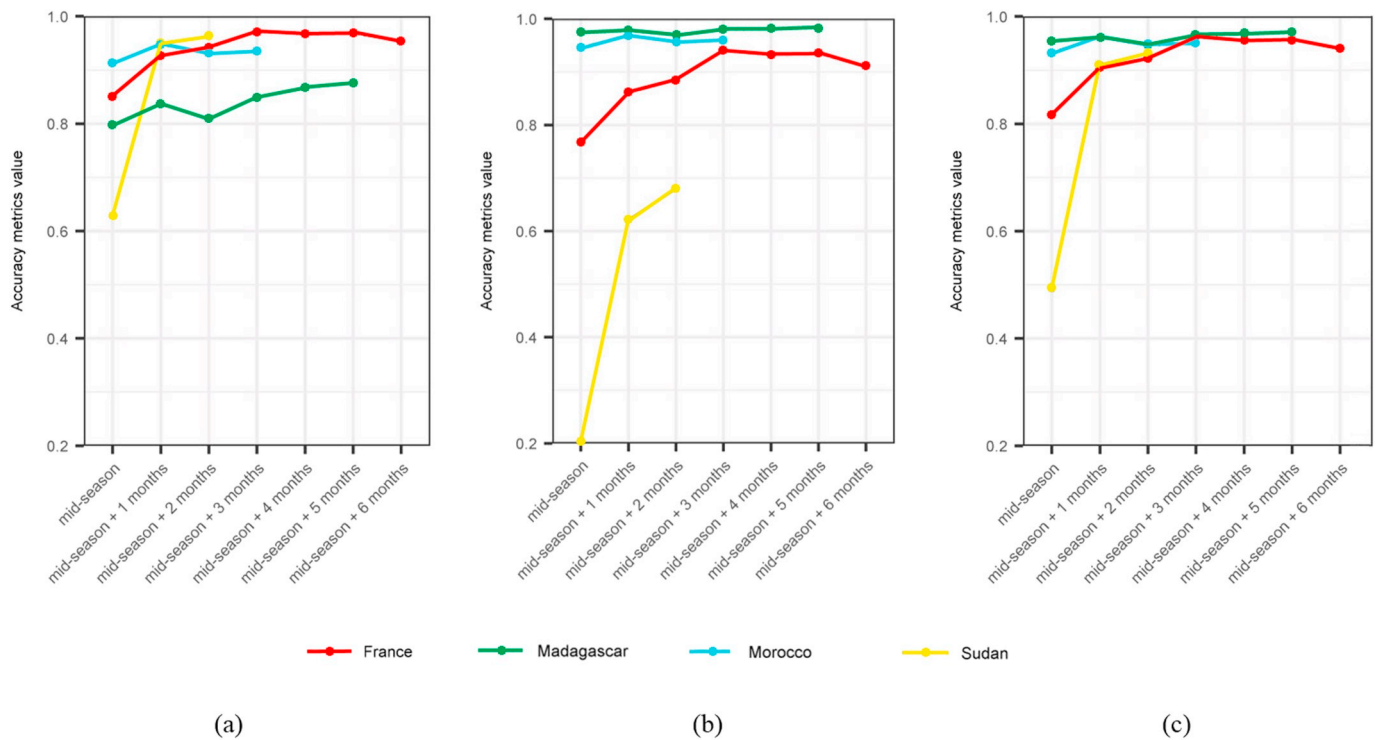
Fig. 11. Evolution of the cropland mask accuracy throughout the growing season over four contrasted local demonstration sites (90,000 km² each) in terms of the (a) F1-Score of the cropland class, (b) F1-Score of the non-cropland class and (c) OA.

Table 5
F1-Scores and OA achieved by the end-of-season cropland masks generated without *in situ* data over the local sites of China, Shandong, France and Sudan and the Ukraine national site.

Site	F1 cropland	F1 non-cropland	OA [%]
China, Shandong	0.92	0.93	92
France, Occitanie	0.87	0.75	84
Sudan, White Nile/South-Sudan	0.87	0.49	79
Sudan, White Nile/South-Sudan (with local LC map)	0.91	0.57	85
Ukraine	0.98	0.87	96

exceptions of "soybean" in Madagascar and "sesame" in Sudan. The "sesame" class proved to be very difficult to classify, being affected by significant omission and commission errors with sorghum, and to a lesser extent with some non-cropland classes. The lower accuracy generally observed in Madagascar can be easily explained by very small field sizes (down to 20 × 20 m), not so compatible with the 10 m resolution of the S2 instrument.

As expected, the mid-season products provide lower accuracy metrics but still reach a quality level already useable for early operational monitoring. The class that suffers most from this early discrimination is the "soybean" in France. Conversely, some specific crops, like "winter rapeseed" in France and "alfalfa" in Morocco, are better identified at the middle of the season than at the end, most probably because of their specific crop calendar.

4.4. Vegetation status maps

Unlike the other Sen2-Agri products, NDVI and LAI maps were continuously generated over all sites for each S2 and L8 image acquired with less than 90% of cloud cover. These NDVI and LAI time series provide the evolution of the green vegetation in near real-time. They can be masked with the Sen2-Agri cropland masks or crop type maps to

highlight the growing condition of all crops or of a specific crop vegetation, as illustrated in Fig. 13 for winter wheat fields in Ukraine.

5. Discussion

This research demonstrated the utility of the Sen2-Agri system for large-scale agriculture monitoring in various cropping systems widely distributed over the world. It provided quantitative results over three entire countries (Ukraine, Mali, South Africa) and five local sites and discussed the performances in relation to analyzed agro-ecosystems and quality of *in situ* data.

The cropland and crop type maps generated with *in situ* data show that all the crops could be mapped with the Sen2-Agri system. It is however important to mention that only the main crops were considered during this study. Minor and marginal crops would require special attention for their respective representativeness in the calibration as well as in the validation dataset. From the experiments carried out in this study, it could be recommended to collect, for the calibration dataset, between 75 and 100 samples for each main crop and between 20 and 30 samples for each minor crop, for each stratum. Yet, these figures need to be interpreted cautiously, since it really depends on each site characteristic.

To some extent, the crop type mapping accuracy is driven by the crop calendar. Crop types are classified twice along the season, at the middle and at the end. The legend is the same for both periods, including crops with very different calendars and growing cycles. Lower mapping accuracy values can therefore come from the fact that some crops are not easily discriminated at the specific periods corresponding to the middle and the end of the season. Over the French site for instance, it was the case for (i) the soybean which is planted in April–May and which is logically not well discriminated in the map from the end of May and (ii) the winter rapeseed which is harvested in July and thus better mapped in May than at the end of the season, defined as the 30th of November. Alfalfa in Morocco is harvested several times during the year and is therefore also challenging to discriminate accurately. A first solution to deal with the variety of crop calendars might come from the
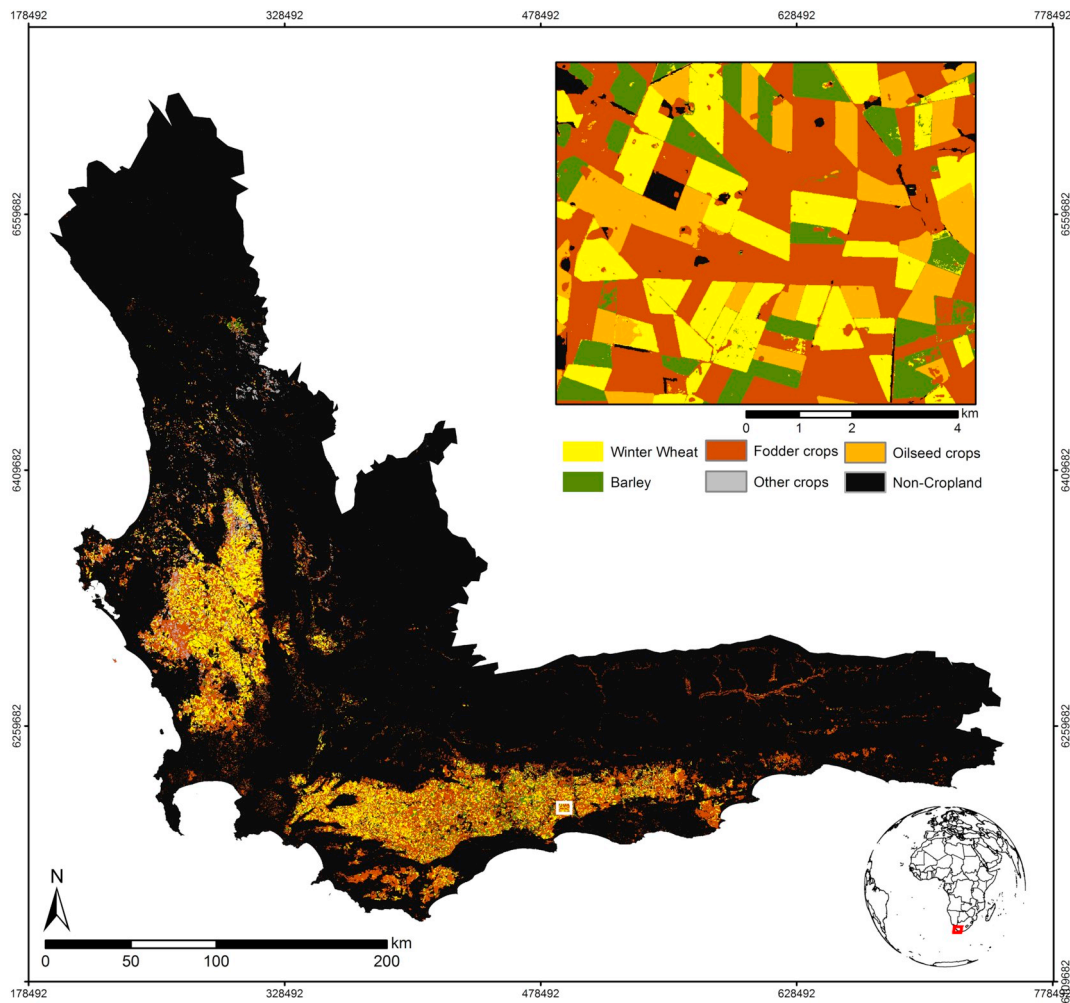
Fig. 12. 10 m crop type map for 2016 over Western Cape, the main winter grain production region in South Africa.

Table 6
F1-Scores and OA achieved by the end-of-season crop type map over three national demonstration sites.

	F1 crop type					OA [%]
Ukraine	Winter wheat	Sunflower	Maize	Winter barley	Soybean	82.7
	0.88	0.88	0.85	0.29	0.67	
South Africa – WGR	Winter wheat	Fodder crops	Oilseed crops	Winter barley		81.2
	0.84	0.82	0.93	0.68		
South Africa – SGR	Maize	Sunflower	Soybean			90.1
	0.94	0.82	0.83			

use of different legends between mid- and end-of-season products to reflect what is effectively visible on the ground. A mid-season crop type map could focus on the discrimination of summer *vs* winter crops, of irrigated *vs* rainfed crops and of crops which are fully developed at that stage while the end-of season map could provide the detailed "crop specific" legend. A second solution would be to increase the flexibility for the dates at which the crop type maps are generated, either by manually defining the dates or by increasing the number of the maps along the season. Like for the cropland mask, which is generated every month from the mid-season, it would thus be the responsibility of the user to select the best product to use depending on a specific application.

More generally, the good accuracy estimates obtained for crop mapping can be related with the performance of the methods developed

to specifically address large-scale agriculture monitoring applications, with the density and quality of the EO time series and with the quality of *in situ* data collected over each site (quality referring to their accuracy in geolocation and in crop type identification and their spatial sampling regarding agro-climatic conditions and crop types). While these accuracies are rather high by remote sensing standards for crop mapping, they could still be improved by tuning the calibration dataset.

The accuracy figures were obtained using a validation *in situ* dataset spatially independent of the calibration dataset, as each reference polygon was included either in the calibration or validation set. While this is often considered as a product validation as soon as the data are independent, this should be only the case when the validation samples are distributed over the whole area covered by the product. The representativeness of the validation sampling has been carefully designed and completed for all nationwide demonstration where a very comprehensive *in situ* data collection campaign insured the national coverage. Over the local sites, the representativeness of the field sampling plan varied according to logistic and unexpected constraints like political unrest (*e.g.* Madagascar) and flooding events (*e.g.* Sudan). The validation datasets can be considered representative of the entire 300 × 300 km site only over France and Morocco. In the other sites, the accuracy figure should be interpreted in light of the actual spatial distribution of the validation dataset. Because of the automated nature of this validation process fully embedded into the Sen2-Agri system, specific attention to the representativeness of the reference data collection is required as it always delivers accuracy figures, regardless the spatial distribution of the reference data.

Table 7

F1-Scores and OA achieved by the mid of season and end-of-season crop type maps in France, Madagascar, Sudan and Morocco.

		F1 Crop type					OA [%]
France, Occitanie		Maize	Straw cereals	Sunflower	Winter rapeseed	Soybean	
	Mid-season	0.84	0.98	0.82	0.90	0.37	86.3
	End-of-season	0.94	0.98	0.96	0.69	0.60	94.1
Madagascar, Antsirabe		Rice	Maize	Sweet potatoes	Soybean		
	Mid-season	0.66	0.68	0.90	0.34		66.3
	End-of-season	0.69	0.8	0.88	0.34		66.3
Sudan, White Nile/South-Sudan		Sorghum	Sesame				
	Mid-season	0.87	0.20				78.4
	End-of-season	0.91	0.34				84.6
Morocco, Tensift		Winter wheat	Alfalfa	Maize	Sugar beet		
	Mid-season	0.87	0.67	0.61	0.72		82.2
	End-of-season	0.93	0.60	0.78	0.83		89.3

Large-scale agriculture monitoring has to deal with significant agro-climatic gradients and crop calendars diversity and overlapping, making it very difficult to define the start and the end of a growing season. The research introduced the concept of rolling cropland masks based on the last 12 months, with a monthly update. The binary map delivered each month from the middle of the season proved to be capable of capturing cropping calendar shifts along an agro-climatic gradient, as shown with the accuracy evolution of the cropland masks along the season. Yet these masks were generated only during agricultural seasons shorter than one year (see Table 3) and it would be of interest to further investigate its performance all the year round. The stratification *a priori* applied to the area to classify is also a key aspect of the crop mapping strategy, allowing dealing with the S2 wide-swath coverage encompassing agro-ecological gradients while being locally relevant thanks to the user knowledge. The too coarse stratification of South Africa had a significant negative impact on the crop type classification because it forced to consider, all together, too many different management systems and agro-ecological conditions. This stratification was applied both for the cropland and crop type classification and ensured high spatial consistency between tiles belonging to a same agro-system.

The unique properties of S2, particularly well-suited for agricultural applications, have also contributed to the promising results of this research. The temporal resolution is the first key asset of S2 for agriculture, even if this study benefitted only from S2A and its 10-day (20-day in China) revisit cycle. The successful launch and operation of the S2B further improves the data availability, thus reducing the gap-filling role of the 30-m Landsat time series, much required for this demonstration. Along with the S2 Global Reference Image enabling a more accurate co-registration between S2 images, the enhanced availability of the S2 data will surely improve the quality of the results as well as their timeliness despite the higher volume of data to process. Such an

evolution should improve the Sen2-Agri performances in cropping systems with very small fields and heterogeneous agriculture landscapes, where even the 10-m resolution time series faces some challenges to capture specific signal for each parcel. It is worth mentioning that the China and the Mali demonstration sites were successfully processed in spite of the majority of smallholder farmers with small fields thanks to the relative homogeneity of the agricultural landscape largely dominated by very few crops. The typical temporal co-occurrence between the crop growing period and rainy season with frequent cloud cover certainly calls for the use of the S2B time series to enhance the reliability of observations availability. Table 3 provided a first insight of the regions and periods within the year for which it is challenging to get enough cloud-free observations. In some regions, it is expected that only the all-weather observation capacity currently provided by the Sentinel-1 constellation could reach the required level of observation reliability to ensure timeliness, in particular for mid-season cropland mask and crop type maps. In spite of the very different nature of the active microwaves signal, SAR-derived features can indeed be jointly used with optical features for classification purpose (Hütt et al., 2016; Kussul et al., 2014; Navarro et al., 2016).

The collection of high quality *in situ* data according to a statistically sound sampling design over a large-scale region and their quality control in a timely manner is a significant challenge. The accuracy of the LAI products has not been assessed locally for the different study sites because of the lack of resources. Yet, this would be relevant at least once to support appropriate products uses. This requires measuring *in situ* a set of fields of each main crop about 4 to 6 times over the growing cycle to sample the full values range of the biophysical variables in actual farms fields. It is important to mention that the remotely sensed LAI estimate concerns all plants observed in a pixel including weeds, hedges and possibly trees as it is the case in Mali.

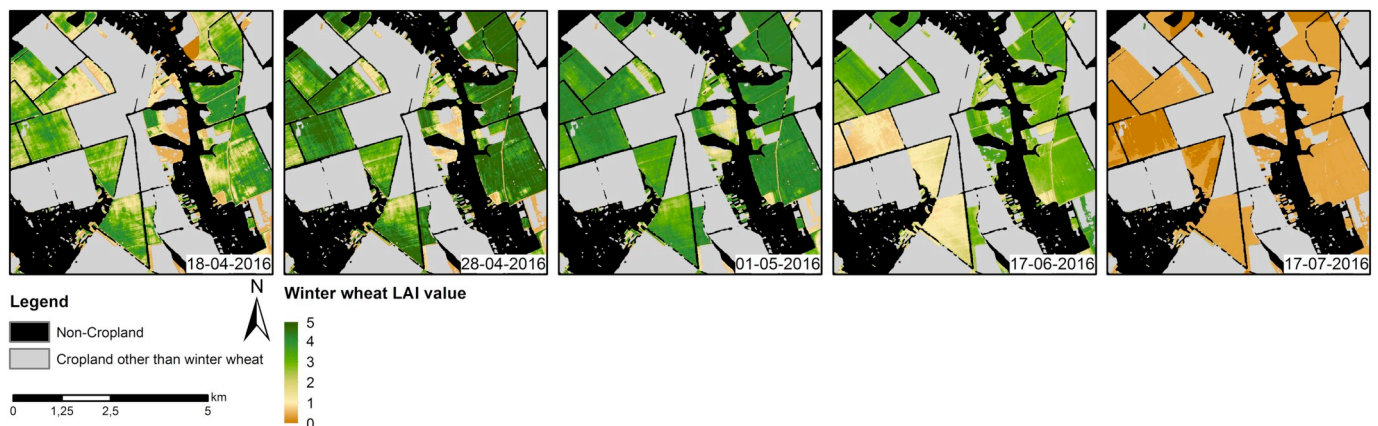Another key challenge about *in situ* data is related to the near-real

Fig. 13. Crop specific monitoring at parcel level based on the LAI evolution: zoom on some winter wheat fields extracted from the national LAI maps of Ukraine.

time operation and the need for their timely provision. As already mentioned, the near-real time conditions were only tested in South Africa while the other case studies were retrospective exercises. Near-real time production requires two delivery of *in situ* data representative from the cropland and crop type classes at the middle and at the end of the season. A unique *in situ* data set is enough for the non-cropland class, assuming it does not change during the year. These constraints were fully met for the demonstration in South Africa and it allowed delivering the first cropland mask and the first crop type map respectively 5 days and 2 weeks after the mid-season date. In the other case studies, the same *in situ* dataset was used for the generation of all products during the season.

It is worth mentioning that the Sen2-Agri system partly responded to the difficulty of getting reliable *in situ* data, with the development of an unsupervised algorithm for cropland mapping. Collection of *in situ* data might become a problem for varying reasons: data not available before the end of the season while early estimates are needed, sites just starting to develop monitoring capabilities using remote sensing data which will need a few seasons to learn and get reliable field data, and most importantly, sites over which field data is never available for security reasons, which are typically the ones concerned by food security issues. The method was successfully validated, with promising results even if the accuracy estimates are logically a bit lower than the ones obtained using *in situ* data. OA values were still higher than 80% and F1-Score for cropland and non-cropland classes higher than 0.75. As for the *in situ* data, the quality of the classification is driven by the quality of the reference map used to extract training samples. The by-default map is a global land cover map from 2010 at 300-m spatial resolution. The use of a more recent map and/or with a higher spatial resolution, better matching the 10-m S2 data will surely improve the quality of the results. A local map, will also help a lot, because of (i) a more meaningful legend better capturing the local landscape patterns and (ii) hopefully, a higher accuracy over the specific area to map.

The processing related to these demonstrations over the three national and five local sites was implemented on a cloud computing infrastructure. The scalability of the Sen2-Agri system allowed handling unusual remote sensing data flows in a near real-time manner. This system delivered for the very first time nationwide 10 m resolution products for several countries within the year of observation thanks to a very high level of automation. It should be mentioned that the near real-time specification was only fully met for the Southern Hemisphere sites (South Africa and Madagascar) thanks to the lessons learnt from the Northern Hemisphere experiences in the previous months, which was the first with S2 coverage acquired and available during the crop season. In addition to the processing performances, the timeliness of the large-scale *in situ* data collection and the necessary quality control were also identified as significant bottlenecks for near real-time delivery. In South Africa, the Sen2-Agri products for the large WGR were delivered early May 2017 for the agriculture season ending late April. In a cloud-computing environment, the most demanding processing module requires only up to 5 days for a 500,000 km^2 country because the surface reflectance time series are calibrated, cloud screened and atmospherically corrected along their availability.

These full-scale achievements were made possible thanks to the development of the very first open source operational system providing large scale near real-time production capabilities using the full time series of S2 and L8. The full integration of the different workflows from download to validation was found instrumental for large-scale operational production but this comes at the cost of limited flexibility. Unlike toolbox providing a choice of algorithms for every processing step, the Sen2-Agri system is optimized for predefined sequences of operations and only few intermediary products are stored to reduce the required storage capacity.

Two main operation modes are available in the system providing some flexibility:

- an automated mode, in which S2 L1C and/or L8 L1T data are downloaded as they become available, and the processing chains are scheduled to execute accordingly;
- a user-oriented mode, in which a human operator can trigger the execution of any of the processing chains *via* a friendly user interface with custom configuration parameters.

The Sen2-Agri system along with Software User Manual and product description sheets are available for download since July 2017 (WWW3). Next versions of the Sen2-Agri system is expected to use the new version of MACCS, renamed MAJA (for MACCS-ATCOR Joint Algorithm) (MAJA, 2017).

6. Conclusion

The proposed key principles for high-resolution crop specific monitoring at national scale allows addressing the new challenges associated to the processing of agricultural vegetation observation at 10 m, over large-scale regions from various orbits associated to different platforms and instruments. The automated processing design taking advantage of cloud computing infrastructure successfully met the near real-time requirements in spite of the volume of dense time series covering up to national territories. Thanks to the quality of the S2 and L8 observations, the four top priority products requested by many end-users have been successfully demonstrated for a set of cropping systems around the world. The automated orchestrator releases the burden of big EO data processing associated to the high spatial and temporal resolution of the current observing systems. The open source Sen2-Agri system was designed and implemented to enable agriculture monitoring in most countries. However, this system, based only on decametric optical observations, will face major constraints in the agricultural regions very frequently covered by clouds during the growing season, made of very small fields (less than 0.5 ha) or with mixed cropping in many fields. While the system runs automatically, products performances vary according to the temporal distribution of the S2 and L8 observations and to the spatial distribution of quality-controlled *in situ* data collected during the season.

The high uptake of the Sen2-Agri system by different operational stakeholders confirms its relevance to support national monitoring like in Ukraine, to enhance official agriculture statistics as experienced in Mali, and for commercial agriculture outcome management like in South Africa. The potential or actual availability of these basic agriculture products requested for a long time by many stakeholders, calls now for the development of specific expertise to assess at high resolution the emergency in food insecure countries, to report agriculture production for the SDG-2, and to develop EO monitoring capacities at national to regional scale as promoted by the GEOGLAM initiative.

Appendix A. Supplementary data

Supplementary data to this article can be found online at https://doi.org/10.1016/j.rse.2018.11.007.

References

Biradar, C.M., Thenkabail, P.S., Noojipady, P., Li, Y., Dheeravath, V., Turral, H., Velpuri, M., Gumma, M.K., Gangalakunta, O.R.P., Cai, X.L., et al., 2009. A global map of rainfed cropland areas (GMRCA) at the end of last millennium using remote sensing. Int. J. Appl. Earth Obs. Geoinf. 11, 114–129.

Blaes, X., Vanhalle, L., Defourny, P., 2005. Efficiency of crop identification based on optical and SAR time series. Remote Sens. Environ. 96, 352–365.

Bogovin, A.V., 2001. Country Pasture/Forage Resource Profiles in Ukraine. FAO.

Bontemps, S., Arias, M., Cara, C., Dedieu, G., Guzzonato, E., Hagolle, O., Inglada, J., Matton, N., Morin, D., Popescu, R., et al., 2015. Building a Data Set over 12 Globally Distributed Sites to Support the Development of Agriculture Monitoring Applications with Sentinel-2. Remote Sens. 7, 16062–16090.

Boryan, C., Yang, Z., Mueller, R., Craig, M., 2011. Monitoring US agriculture: the US Department of Agriculture, National Agricultural Statistics Service, cropland data layer program. Geocarto Int. 26, 341–358.

Bréon, F.M., Vermote, E.F., 2012. Correction of MODIS surface reflectance time series for BRDF effects. Remote Sens. Environ. 125 (1–9).

Davidson, A.M., Fisette, T., Mcnairn, H., Daneshfar, B., 2017. Detailed crop mapping using remote sensing data (Crop Data Layers). In: Delincé, J. (Ed.), Handbook on Remote Sensing for Agricultural Statistics (Chapter 4). FAO Handbook of the Global Strategy to improve Agricultural and Rural Statistics (GSARS), Rome, pp. 91–117.

Desclée, B., Bogaert, P., Defourny, P., 2006. Forest change detection by statistical object-based method. Remote Sens. Environ. 102, 1–11.

Doxani, G., Vermote, E., Roger, J.C., Gascon, F., Adriaensen, S., Frantz, D., Hagolle, O., Hollstein, A., Kirches, G., Li, F., Louis, J., Mangin, A., Pahlevan, N., Pflug, B., Vanhellemont, Q., 2018. Atmospheric correction inter-comparison exercise. Remote Sens. 10, 352.

ESA Sentinel-2 for Agriculture, 2016. Design Definition File. v1.2., Available online at. http://www.esa-sen2agri.org/wp-content/uploads/resources/technical-documents/Sen2-Agri-Design-Definition-File-1.2.pdf, Accessed date: 8 February 2018.

Feret, J.B., Francois, C., Asner, G.P., Gitelson, A.A., Martin, R.E., Bidel, L.P.R., Ustin, S.L., le Maire, G., Jacquemoud, S., 2008. PROSPECT-4 and 5: advances in the leaf optical properties model separating photosynthetic pigments. Remote Sens. Environ. 112, 3030–3043.

Fisette, T., McNairn, H., Davidson, A., 2015. An Operational Annual Space-based Crop Inventory Based on the Integration of Optical and Microwave Remote Sensing Data: Protocol Document. Agriculture and Agri-Food Canada Publication, Ottawa.

Fritz, S., See, L., Laso Baya, J.C., Waldner, F., Jacques, D., Becker-Reshef, I., Whitcraft, A., Baruth, B., Bonifacio, R., Crutchfield, J., Rembold, F., Rojas, O., Schucknechti, A., Van der Velde, M., Verdin, J., Wu, B., Yan, N., You, L., Gilliams, S., Mücher, S., Tetrault, R., Moorthy, I., McCallum, I., 2018. A comparison of global agricultural monitoring systems and current gaps. Agric. Syst. 168, 258–272.

Gascon, F., Bouzinac, C., Thépaut, O., Jung, M., Francesconi, B., Louis, J., Lonjou, V., Lafrance, B., Massera, S., Gaudel-Vacaresse, A., et al., 2017. Copernicus sentinel-2A calibration and products validation status. Remote Sens. 9, 584.

Genovese, G., Vignolles, C., Nègre, T., Passera, G., 2001. A methodology for a combined use of normalised difference vegetation index and CORINE land cover data for crop yield monitoring and forecasting. A case study on Spain. Agronomie 21 (1), 91–111.

Gitelson, A., Merzlyak, M.N., 1994. Spectral Reflectance Changes Associated with Autumn Senescence of *Aesculus hippocastanum* L. and *Acer platanoides* L. Leaves. Spectral Features and Relation to Chlorophyll Estimation. J. Plant Physiol. 143 (3), 286–292.

Grizonnet, M., Michel, J., Poughon, V., Inglada, J., Savinaud, M., Cresson, R., 2017. Orfeo ToolBox: open source processing of remote sensing images. Standards 2, 15.

Hagolle, O., Dedieu, G., Mougenot, B., Debaecker, V., Duchemin, B., Meygret, A., 2008. Correction of aerosol effects on multi-temporal images acquired with constant viewing angles: application to Formosat-2 images. Remote Sens. Environ. 112, 1689–1701.

Hagolle, O., Huc, M., Villa Pascual, D., Dedieu, G., 2010. A multi-temporal method for cloud detection, applied to FORMOSAT-2, VENµS, LANDSAT and SENTINEL-2 images. Remote Sens. Environ. 114, 1747–1755.

Hagolle, O., Huc, M., Dedieu, G., Sylvander, S., Houpert, L., Leroy, M., Clesse, D., Daniaud, F., Arino, O., Koetz, B., Paganini, M., Seifert, F.M., Pinnock, S., Hoersch, B., Bartholomé, E., Achard, F., Mayaux, P., Masek, J., Claverie, M., Vermote, E.F., Fernandes, R., 2013. SPOT4 (TAKE 5) time series over 45 sites to prepare Sentinel-2 applications and methods. In: Proceedings of the ESA's Living Planet Symposium, Edinburgh, Scotland, 9–13 September 2013.

Hagolle, O., Sylvander, S., Huc, M., Claverie, M., Clesse, D., Dechoz, C., Lonjou, V., Poulain, V., 2015. SPOT4 (Take5): a simulation of Sentinel-2 time series on 45 large sites. Remote Sens. 7, 12242–12264.

Hatfield, J.L., Prueger, J.H., 2010. Value of using different vegetative indices to quantify agricultural crop characteristics at different growth stages under varying management practices. Remote Sens. 2, 562–578.

Hütt, C., Koppe, W., Miao, Y., Bareth, G., 2016. Best accuracy land use/land cover (LULC) classification to derive crop types using multitemporal, multisensor, and multi-polarization SAR satellite images. Remote Sens. 8, 684.

Inglada, J., Arias, M., Tardy, B., Hagolle, O., Valero, S., Morin, D., Dedieu, G., Sepulcre, G., Bontemps, S., Defourny, P., Koetz, B., 2015. Assessment of an Operational System for Crop Type Map Production Using High Temporal and Spatial Resolution Satellite Optical Imagery. Remote Sens. 7, 12356–12379.

Jacquemoud, S., Verhoef, W., Baret, F., Bacour, C., Zarco-Tejada, P., Asner, G.P., François, C., Ustin, S., 2009. PROSPECT + SAIL models: a review of use for vegetation characterization. Remote Sens. Environ. 113, 56–66.

Johnson, D.M., 2014. An assessment of pre-and within-season remotely sensed variables for forecasting corn and soybean yields in the United States. Remote Sens. Environ. 141, 116–128.

Joint Experiment of Crop Assessment and Monitoring (JECAM), 2018. JECAM Guidelines for cropland and crop type definition and field data collection. Available online at. http://jecam.org/wp-content/uploads/2018/10/JECAM_Guidelines_for_Field_Data_Collection_v1_0.pdf, Accessed date: 29 October 2018.

JRC (Joint Research Center), 2001. In: Leo, O., Lemoine, G. (Eds.), Land Parcel Identification Systems in the Frame of Regulation (EC) 1593/2000 Version 1.4 (Discussion Paper). European Commission Directorate General JRC Joint Research Centre – ISPRA Space Applications Institute Agriculture and Regional Information Systems Unit, pp. 27.

Koetz, B., Baret, F., Poilvé, H., Hill, J., 2005. Use of coupled canopy structure dynamic and radiative transfer models to estimate biophysical canopy characteristics. Remote Sens. Environ. 95, 115–124.

Kussul, N., Skakun, S., Shelestov, A., Kussul, O., 2014. The use of satellite SAR imagery to crop classification in Ukraine within JECAM project. In: Proceedings of the IEEE Geoscience and Remote Sensing Symposium, Quebec City, QC, Canada, 13–18 July 2014.

Lambert, M.-J., Waldner, F., Defourny, P., 2016. Cropland mapping over Sahelian and Sudanian Agrosystems: a knowledge-based approach using PROBA-V time series at 100-m. Remote Sens. 8, 232.

Land Cover CCI, 2017. Product User Guide, version 2.0, ref: CCI-LC-PUGV2. Available online at. http://maps.elie.ucl.ac.be/CCI/viewer/download/ESACCI-LC-Ph2-PUGv2_2.0.pdf, Accessed date: 22 December 2017.

Li, X., Strahler, A.H., 1992. Geometric-optical bidirectional reflectance modeling of the discrete crown vegetation canopy: effect of crown shape and mutual shadowing. IEEE Trans. Geosci. Remote Sens. 30, 276–292.

Lussem, U., Hütt, C., Waldhoff, G., 2016. Combined analysis of Sentinel-1 and RapidEye data for improved crop type classification: an early season approach for rapeseed and cereals. ISPRS XLI-B8, 959–963.

Maignan, F., Breon, F.-M., Lacaze, R., 2004. Bidirectional reflectance of earth targets: evaluation of analytical models using a large set of spaceborne measurements with emphasis on the hot spot. Remote Sens. Environ. 90, 210–220.

MAJA, 2017. Algorithm Theoretical Basis Document, ref: MAJA-TN-WP2-030 V1.0 2017/Dec/07. Available online at. http://tully.ups-tlse.fr/olivier/maja_atbd/blob/master/atbd_maja.pdf, Accessed date: 22 December 2017.

Matton, N., Sepulcre Canto, G., Waldner, F., Valero, S., Morin, D., Inglada, J., Arias, M., Bontemps, S., Koetz, B., Defourny, P., 2015. An Automated Method for Annual Cropland Mapping along the Season for Various Agrosystems Globally Distributed Using Spatial and Temporal High Resolution Time Series. Remote Sens. 7, 13208–13232.

McNairn, H., Champagne, C., Shang, J., Holmstrom, D., Reichert, G., 2009. Integration of optical and Synthetic Aperture Radar (SAR) imagery for delivering operational annual crop inventories. ISPRS J. Photogramm. Remote Sens. 64, 434–449.

Merzlyak, M.N., Gitelson, A.A., Chivkunova, O.B., Rakitin, V.Y., 1999. Non-destructive optical detection of pigment changes during leaf senescence and fruit ripening. Physiol. Plant. 106, 135–141.

Navarro, A., Rolim, J., Miguel, I., Catalao, J., Silva, J., Painho, M., Vekerdy, Z., 2016. Crop monitoring based on SPOT-5 Take-5 and sentinel-1A data for the estimation of crop water requirements. Remote Sens. 8, 525.

Parihar, J.S., Justice, C.O., Soares, J., Leo, O., Kosuth, P., Jarvis, I., Williams, D., Bingfang, W., Latham, J., Becker-Reshef, I., 2012. GEO-GLAM: A GEOSS-G20 initiative on global agricultural monitoring. In: Proceedings of the 39th COSPAR Scientific Assembly, Mysore, India, 14–22 July 2012.

Radoux, J., Lamarche, C., Van Bogaert, E., Bontemps, S., Brockmann, C., Defourny, P., 2014. Automated training sample extraction for global land cover mapping. Remote Sens. 6, 3965–3987.

Ray, S.S., Neetu, Manjunath, K.R., Singh, K.K., 2016. Crop production forecasting using space, agrometeorology and land based observations: Indian experience. In: Paper Presented at the International Seminar on Approaches and Methodologies for Crop Monitoring and Production Forecasting, 25–26 May 2016, Dhaka.

Ross, J., 1981. The Radiation Regime and Architecture of Plant Stands. Artech House, Norwood, MA, USA.

Roy, D.P., Zhang, H.K., Ju, J., Gomez-Dans, J.L., Lewis, P.E., Schaaf, C.B., Sun, Q., Li, J., Huang, H., Kovalskyy, V., 2016. A general method to normalize Landsat reflectance data to nadir BRDF adjusted reflectance. Remote Sens. 176, 255–271.

USDA National Agricultural, 2018. Statistics Service Cropland Data Layer. 2018. Published crop-specific data layer [Online]. Available online at. https://nassgeodata.gmu.edu/CropScape/, Accessed date: 25 July 2018 USDA-NASS, Washington, DC.

Valero, S., Morin, D., Inglada, J., Sepulcre, G., Hagolle, O., Arias, M., Dedieu, G., Bontemps, S., Defourny, P., Koetz, B., 2016. Production of a Dynamic Cropland Mask by Processing Remote Sensing Image Series at High Temporal and Spatial Resolutions. Remote Sens. 8, 55.

Vancutsem, C., Bicheron, P., Cayrol, P., Defourny, P., 2007a. Performance assessment of three compositing strategies to process global ENVISAT MERIS time series. Can. J. Remote. Sens. 33 (6), 492–502.

Vancutsem, C., Pekel, J.-F., Bogaert, P., Defourny, P., 2007b. Mean compositing, an alternative strategy for producing temporal syntheses. Concepts and performance assessment for SPOT VEGETATION time series. Int. J. Remote Sens. 28 (22), 5123–5141.

Vancutsem, C., Marinho, E., Kayitakire, F., See, L., Fritz, S., 2012. Harmonizing and combining existing land cover/land use datasets for cropland area monitoring at the African continental scale. Remote Sens. 5, 19–41.

Waldner, F., De Abelleyra, D., Veron, S.R., Zhang, Miao, Wu, Bingfang, Plotnikov, D., Bartalev, S., Lavreniuk, M., Skakun, S., Kussul, N., Le Maire, G., Dupuy, S., Jarvis, I., Defourny, P., 2016. Towards a set of agrosystem-specific cropland mapping methods

to address the global cropland diversity. Int. J. Remote Sens. 37 (14), 3196–3231.

Weiss, M., Baret, F., Leroy, M., Hautecoeur, O., Bacour, C., Prévot, L., Bruguier, N., 2002. Validation of Neural Net techniques to estimate canopy biophysical variables from remote sensing data. Agronomie 22 (6), 547–553.

Whitcraft, A.K., Becker-Reshef, I., Justice, C.O., 2015a. A framework for defining spatially explicit earth observation requirements for a global agricultural monitoring initiative (GEOGLAM). Remote Sens. 7, 1461–1481.

Whitcraft, A.K., Becker-Reshef, I., Killough, B.D., Justice, C.O., 2015b. Meeting Earth Observation Requirements for Global Agricultural Monitoring: an Evaluation of the Revisit Capabilities of Current and Planned Moderate Resolution Optical Earth Observing Missions. Remote Sens. 7, 1482–1503.

Xu, X., Doktor, D., Conrad, C., 2016. Phenological metrics extraction for agricultural land-use types using RapidEye and MODIS. Geophys. Res. Abstr. 18, 10375.

Yan, L., Roy, D.P., 2014. Automated crop field extraction from multi-temporal web en-abled Landsat data. Remote Sens. Environ. 144, 42–64.

References to websites

ACIX Atmospheric Correction Inter-comparison eXercise portal. http://calvalportal.ceos.org/projects/acix, Accessed date: 26 July 2018.

ESA Sentinel-2 Toolbox. http://step.esa.int/main/toolboxes/sentinel-2-toolbox/, Accessed date: 29 October 2018.

ESA Sentinel-2 for Agriculture. http://www.esa-sen2agri.org/, Accessed date: 24 July 2018.

FARMSTAR service http://www.farmstar-conseil.fr, Accessed date: 24 July 2018.

Joint Experiment of Crop Assessment and Monitoring (JECAM) http://jecam.org/, Accessed date: 25 October 2018.

MasAgro GreenSat project. http://www.cmgs.gob.mx:8080/ddr/ndvi.aspx, Accessed date: 24 July 2018.

FAOSTAT portal Food and agricultural data. http://www.fao.org/faostat/en/, Accessed date: 30 November 2018.

OTB Orfeo ToolBox. https://www.orfeo-toolbox.org/, Accessed date: 13 October 2017.